ThermoFisher
SCIENTIFIC

Spectroscopy and Materials Characterization Applications for Pharmaceutical Analysis

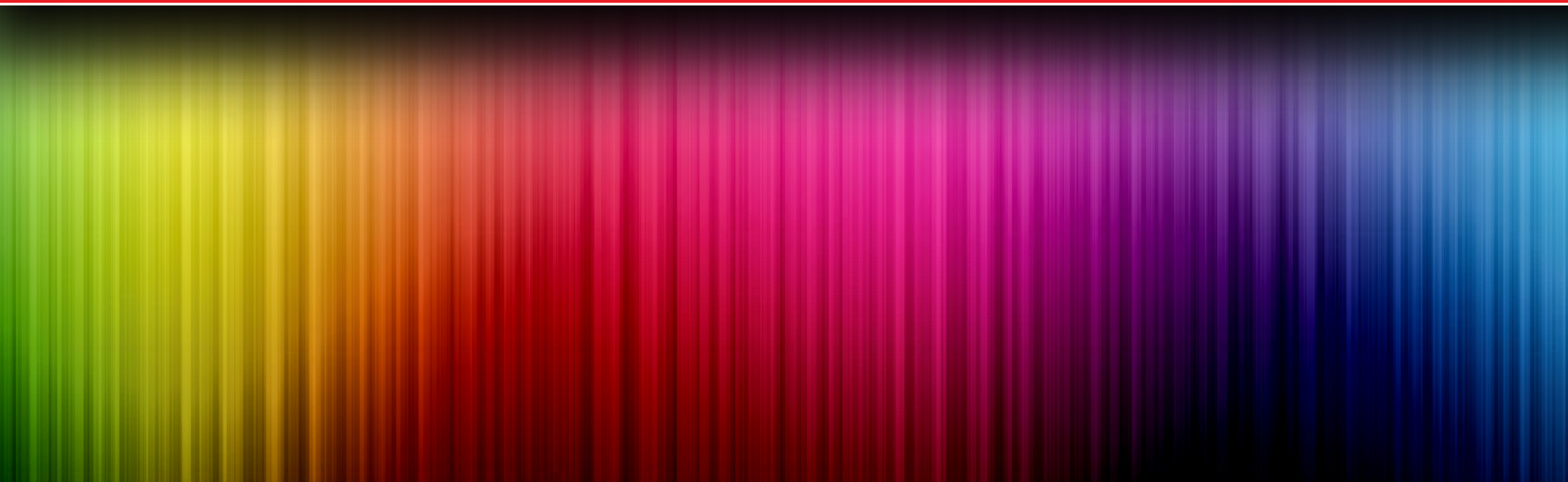

Introduction

Spectroscopy and materials characterization applications for pharmaceutical analysis

During the drug development pipeline, pharmaceutical manufacturers face numerous challenges associated with formulation, scale-up and quality control. A deep understanding of these challenges is key to enable the quick delivery of next-generation drugs to market.

Thermo Fisher Scientific has innovative solutions at every stage of the development process, including discovery, development, clinical, manufacturing and quality control. This ebook contains a series of posters specifically focusing on drug formulation, scale-up and analysis; quality control and validation; and nucleic acid quantification and qualification.

Formulation

As the industry transitions from inefficient batch processing to continuous manufacturing, compounding and extrusion technologies have become a valuable tool in creating novel drug formulations. Extruders and related analytical instrumentation can help provide the shortest path from feasibility studies to production in drug formulation and manufacturing.

Analysis

Pharmaceutical analysis, performed using spectroscopic and microscopic analytical instruments, provides feedback in the form of a spectrum that identifies a material or flags an unknown compound such as a contaminant or inclusion. These tools are used to help ensure quality from early research through formulation and final production.

Nucleic acid quantification

Experiments that use nucleic acids require that the concentration and purity of the sample is known. Instrumentation that can identify contaminants and obtain corrected concentrations to confirm samples are qualified for downstream applications.

For further information relating to any of the posters or Thermo Fisher Scientific's product offerings, please visit:
www.thermofisher.com

Contents

Drug formulation, scale-up, and analysis

Resources

Quality control and validation

Nucleic acid quantification and qualification

Drug formulation, scale-up, and analysis

Investigating process parameter mechanism for successful scale-up of a hot melt extrusion process

Katharina Paulsen[1], Andreas Gryczke[2], and Dirk Leister[1] – [1]Thermo Fisher Scientific, Karlsruhe, Germany and [2]BASF SE, Lampertheim, Germany

INTRODUCTION

Hot melt extrusion (HME) is a suitable process to produce a wide range of pharmaceutical dosage forms, like tablets, capsules, lozenges, or implants. HME can be used for immediate release as well as for sustained release formulations.

Like freeze drying or spray drying, the melt extrusion process is used to achieve solid dispersions, which means that the drug is embedded in a polymeric carrier. In this solid dispersion the drug can be dispersed into the crystalline or amorphous state or it can be dispersed on a molecular level in the polymer. In case of a molecular dispersed drug in the carrier this solid solution may result in an increase of solubility, dissolution rate, and also bioavailability. Because of more and more poorly soluble drugs coming from the high throughput screening of drug development departments into the formulation development laboratories, the hot melt extrusion process is rapidly gaining interest. Since melt extrusion is still a relatively new process for the pharmaceutical industries it is more often used for formulation development than in the production environment yet. To handle such a continuous melt extrusion process, it is absolutely necessary to understand the influence of the variables process parameters on the resulting process parameters and your final product.[1, 2]

Overview of parallel twin screw extruders (top: Pharma11 with 11 mm, middle: Pharma 16 with 16 mm, and bottom: Pharma 24 with 24 mm screw diameter)

The purpose of this work was to get a deeper understanding of the influence of process parameters on the residence time distribution of the material within the extruder and the specific mechanical energy consumption (SMEC) and to determine the possibilities of up scaling this process from a lab scale to a production line extruder. To save development time and material the opportunity of predictability of the scaleup step was determined with a design of experiments approach. Therefore Soluplus® was extruded on three different sizes of a co-rotating twin-screw compounder, in different process settings following a design-of-experiments plan. As important process parameters, the residence time distribution was measured with a tracer in each setup and the specific mechanical energy consumption were calculated. Beside these special process parameters all standard parameters (e.g., temperature of the melt at the extruder die, pressure at the die, and torque) were measured as well.

From the residence time distribution, the mean residence time was calculated. Residence time distribution was obtained by measuring the concentration of a color pigment with a photometric and a colorimetric method. The data of the three independent design-of-experiments were analyzed in an analysis of variance (ANOVA) and the resulting multi-dimensional regression models were used to calculate the design spaces, which are compared for their overlap between the different scales of the extruders.

MATERIAL AND METHODS

Material

Soluplus® is used as a polymeric carrier. It is a polyvinylcaprolactam–polyvinylacetate–polyethyleneglycol graft copolymer (BASF SE, Ludwigshafen, Germany) with an amphiphilic structure that was developed specifically for increasing the solubility of poorly soluble substances via the HME process. Ferric trioxide is used as a tracer, because of its intensive red color.

Parallel, co-rotating twin screw extruders

Three different sizes of parallel twin screw extruders are used to simulate the scalability of the HME process: for a labscale extruder a Pharma 11, for medium scale a Pharma 16 and for production scale a Process 24 (Thermo Fisher Scientific, Karlsruhe, Germany) are used. The index describes the screw diameter. All barrels have a length of 40 L/D. The settings were varied to a minimum, midpoint, and maximum value for the screw speed (100 rpm, 300 rpm, and 500 rpm), the temperature program (130 °C, 165 °C and 200 °C), and the feed rate (Table 1).

Table 1. Different feed rates used on a different twin screw extruder sizes.

Throughput [kg/h]	min	mid	max
Pharma 11	0,17	1,33	2,40
Pharma 16	0,50	4,00	7,50
Process 24	1,13	6,60	12,00

The feed rate for the different extruder sizes is calculated in dependence on the equation of Schuler (Equation 1).[3]

$$\dot{m}_P = \left(\frac{D_P}{D_L}\right)^3 \cdot \dot{m}_L$$

Equation 1. Empirical equation of Schuler

For all the experiments the screw setup was kept constant with two mixing sections (Figure 1).

Measurement of the residence time

The pigment is added as a tracer to the hopper of the feeding section at a given time T0. The color concentration is measured at the die over the time. In the **picture method**, a picture of the strand is taken every 0.2 sec. On every picture a defined size of strand is detected regarding the amount of red pixel (Figure 2). In the **IR method**, ExtruVis 2 is a colorimeter, developed by A. Gryczke. It is measuring inline the concentration of the pigment in the melt at the die exit.

Figure 1. Setup of screws and barrel used for the scaleup experiments on the Pharma 11, Pharma 16, and Process 24 extruders. At the feeding section (right) the Soluplus® and the pigment are added at a given time T0. The degassing section (left) provides atmospheric degassing to allow water vapor to evaporate out of the polymer.

Figure 2. Residence time distribution measurement setup.

Software for data analysis

Visual X-Sel 11.0 (CRGRAPH, C.U. Ronniger, Germany) with a Design of Experiments (DoE) module is used for planning the experiments. For calculation the prediction a module for multi-dimensional regression models is used. The optimization of the calculation was done with MS Excel 2010 (Microsoft).

RESULTS

To have a successful scale up, it is required to have the same experience for the material on the lab scale extruder as on the bigger, production scale extruder. Therefore it is assumed that the residence time of the material within the extruder must be the same, to allow melting and mixing on one hand and to avoid degradation on the other.

Especially when working with very low feed rates, it is necessary to make sure that there is no influence of the tracer itself on the process and therefore on the measurement of the residence time distribution. If we are thinking about the low feed rates of the lab scale 11 mm extruder, where we have only 0,17 kg/h, that means, that every second less then 50 mg is fed into the extruder. When then the amount of tracer is too high then the value for the feed rate will be higher at that moment the tracer is added and therefore also all the other parameters depending on the feed rate will change as well. So it is easy to imagine that the amount of influence the tracer can have. To determine the influence of the tracer concentration, with the same process settings were measured the residence time distribution with different amounts of tracer (Figure 3).

Figure 3. Influence of tracer concentration. Green: 0.1 g, blue: 0.2 g, black: 0.3 g, red: 0.5 g and purple 1.0 g of tracer were added to the Pharma 16 with constant parameter and constant feed rate.

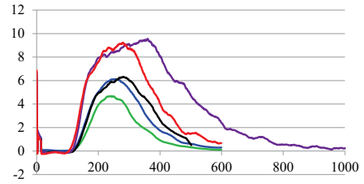

For the scaleup experiments at first, the feed rate was only calculated by the equation of Schuler. As shown in Figure 4, the throughput was increasing from 1 kg/h to 3 kg/h according to this equation when changing from a 11 mm screw diameter to an extruder with 16 mm.

When increasing the feed rate by Schuler the residence time distribution on the next scale extruder is very similar. Nevertheless the distribution is narrower than the distribution of the lab scale extruder and slightly shorter as well. It was found that the residence time distribution is matching perfectly when matching the specific mechanical energy consumption (SMEC).[4]

$$SMEC = \frac{\tau \cdot n}{\dot{m}} \left[\frac{kJ}{kg}\right]$$

τ: torque [Nm]
n: screw speed [rpm]
ṁ: throughput [kg/h]

Equation 2. Calculation of the specific mechanical energy consumption (SMEC)

In the next step the knowledge space of the used extruder sizes is explored with a DoE. Then an ANOVA was performed and the design space was described via multiple regression. Therefore the design space of all the other sizes could be calculated.

The regression model was used to calculate the design space from the 11 mm lab scale to the 24 mm production scale. The regression model was matched regarding residence time, melt temperature, and SMEC (Figure 5).

For the scale up from the design window of the Pharma 11 to the Pharma 16, only the feed rate need to be adjusted to the bigger size. In case of the scale up to a 24 mm system the feed rate needs to be adjusted of course, but also the screw speed needs to be increased as well.

Figure 4. Influence of feed rate and SMEC on the residence time distribution. Orange: lab scale extruder (11 mm), blue: midsize extruder (16 mm), continuous line: feed rate calculated by Schuler, dotted line: feed rate adjusted regarding SMEC.

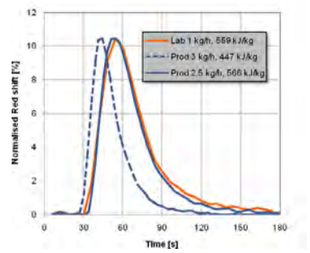

Figure 5. The design space of different sizes twin screw extruder, calculated from the 11 mm scale extruder via regression model.

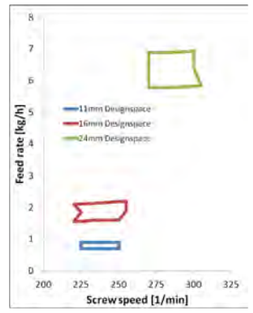

What could be shown here is a limitation of the scaleup process. When increasing the extruder equipment, then the surface area will increase by the power of two. While when the feed rate increases, then this volume will increase by the power of three. So, with increasing extruder size, the ratio between the surface area to introduce heat and cooling energy to the system to the volume of the material is getting smaller. This is why additional energy needs to be added by increasing the screw speed. Also the design space windows are growing with increasing scaleup steps.

Another effect which could be shown in this study is the correlation of the SMEC with the degree of of filling of the extruder (Figure 6). All these effects can be explained by the equation of the SMEC. With increasing feed rate and therefore increasing VSFL there is a decreasing mechanical energy input, because more material share the mechanical energy which is supplied by the system. Another point which is also very important is that with increasing barrel temperatures the SMEC is decreasing. Actually with increasing barrel temperature the viscosity of the material will be decreasing, therefore the torque also will be decreasing. And compared to Equation 2, with decreasing torque the SMEC will decrease as well.

Figure 6. Overview of the correlation between the VSFL and the SMEC. Shown are the figures from Lab to Line extruder equipment (top: 11 mm, middle: 16 mm, bottom: 24 mm). The different colors are linked to different barrel temperatures: Blue: 130 °C, yellow: 165 °C, red: 200 °C.

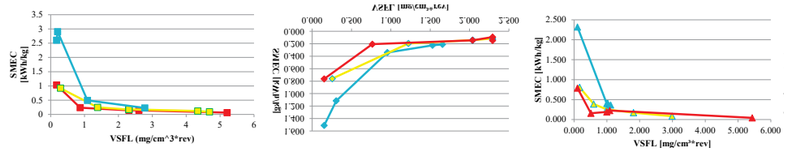

CONCLUSIONS

For each of the three extruder scales a design space could be calculated based on the residence time distribution and the specific mechanical energy consumption.

It could be shown that the residence time distribution and the specific mechanical energy consumption are crucial parameters for an successful scaleup of a pharmaceutical melt extrusion process.

It could be shown the amount of tracer influences the residence time distribution measurement.

REFERENCES

1. Breitenbach, J. Melt extrusion, from process to drug delivery technology, European Journal of Pharmaceutics and Biopharmaceutics, 2002.
2. Douroumis, D. Hot melt Extrusion - Pharmaceutical applications, Willey 2012.
3. Bogun, M. Untersuchungen zur kontinuierlichen Herstellung von Kautschukmischungen basierend auf Rubber/Filler-Composites am Doppelschneckenextruder, Thesis Hallee Germany, 2005.
4. Kohlgrüber, K. Der gleichläufige Doppelschneckenextruder, Carl Hanser Verlag, 2007.

ACKNOWLEDGEMENTS

This work was performed in collaboration with the BASF. In this collaboration the BASF and Thermo Fisher Scientific are working close together to investigate the dependency and influences of process parameters in Hot Melt Extrusion Processes. Also the link between Rheology and HME is investigated.

Especially to understand the process and the way to scale up HME processes are focus of this work.

TRADEMARKS/LICENSING

ThermoFisher SCIENTIFIC

RETURN TO 'CONTENTS' PAGE

A case study of using FT-NIR for pharmaceutical hot melt extrusion process monitoring

Herman He[1], Scott Martin[1], Anh Vo[2], Michael Repka[2], and Rui Chen[1] - Thermo Fisher Scientific, Madison, WI 53711 USA and School of Pharmacy, University of Mississippi, Oxford, MS 38655 USA

ABSTRACT

Incorporating hot melt extrusion (HME) processes into the manufacturing workflow in the pharaceutical industry offers significant benefits for mixing an active pharmaceutical ingredient (API) with a polymer binder to improve its bioavailability and delivery. Stringent monitoring and control of the HME processes and parameters help ensure consistency and quality. Fourier transform near-infrared (FT-NIR) spectroscopy offers a simple method for direct analysis of process samples and can be coupled with chemometrics to develop an appropriate partial least square (PLS) and/or principle component analysis (PCA) model to explore the utility of spectral responses as an indicator for HME process stability.

INTRODUCTION

Continuous manufacturing (e.g., HME), is gaining interest in the pharmaceutical industry due to its high manufacturing efficiency and economic benefits.[1] During HME, which is primarily a mechanical/shear mixing process, an API is melted, mixed, and bonded with thermoplastic polymers and/or other materials. Judiciously designed polymers can promote the bonding structure, improve drug bioavailability, and achieve unique drug delivery profiles.[2, 3, 4] Precise control of HME parameters (screw design, rotational speed, zone temperature, and residence time) is necessary to ensure consistency and product quality, and a thorough understanding of critical parameters is needed to implement an effective process control strategy under the quality by design (QbD) initiative from the FDA.[5, 6]

FT-NIR spectroscopy coupled with statistical regression techniques can provide near real-time chemical information at the molecular level through direct sample measurement. FT-NIR is widely used as a process analytical technology (PAT) and QbD tool for process development and manufacturing to monitor and control drying, blending, extrusion, and more.[7, 8] It is a simple, fast, nondestructive technique for matrix analysis, sensitive to the API concentration in a blend, and can help visualize interactions between the API and its binding polymers. NIR spectra are multivariate in that they are influenced by chemical, physical, and structural properties of all species present. Chemometrics uses mathematical and statistical procedures, such as PLS and PCA, for multivariate data analysis in large datasets. Here we demonstrate the use of FT-NIR for in-line API concentration monitoring during an HME process, discuss the considerations in deriving an appropriate PLS model, and explore the feasibility of employing NIR spectral responses using PCA as an indicator for HME process stability.

METHODS

An 11-mm twin-screw extruder, Thermo Scientific™ Process 11 (Thermo Fisher Scientific) was used for the HME processes. A Thermo Scientific™ Antaris™ II MDS FT-NIR spectrometer (Thermo Fisher Scientific), equipped with a HME diffuse reflectance probe, was used for spectral acquisition. The reflectance probe with standard 1/2-20 UNF mounting threads was screwed into one sensor port of the exit block, between the exhaust gas vent and the exit orifice. To enhance the NIR signal of the hot melt translucent liquid at the sampling location, a metal reflector was placed ~2 mm from the probe on the opposite side. An electric heater controlled by the extruder PLC held the temperature at 120 °C and intentional fluctuations of +/- 10 °C.

Figure 1. Configuration of the Thermo Scientific Process 11 Twin Screw Extruder.

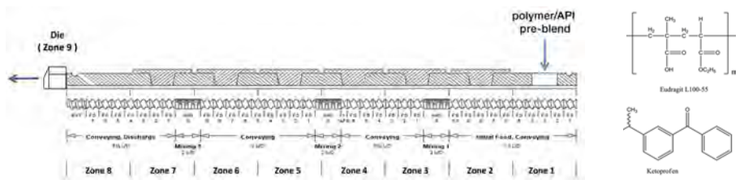

Figure 1 shows screw profile design, process configuration, effective length-to-diameter ratio (L/D), and three mixing zones. Pre-blended polymer (Eudragit® L100-55) and API (ketoprofen) were fed into the extruder at Zone 1. Zones 2 through 8 were mixing, conveying, and discharge zones. The Zone 9 die that reduces the barrel configuration to a single circular orifice.

Experiments were conducted with a 50:50 (w/w) target API:polymer blend, at a temperature of 120 °C (in mixing and melting zones), and at a 100 g/hr feed rate. NIR data were acquired by the Thermo Scientific™ RESULT™ v3 software package (4000–10,000 cm^{-1} spectral range, 8 cm^{-1} resolution, 16 scan average, 8 s/spectrum). The transmission sampling module was used to acquire background reference spectra before each experiment.

RESULTS AND DISCUSSION

Building a PLS model to monitor API concentration for HME

To build a calibration model to predict the API concentration during HME, the pre-blend API/polymer ratio ranged from +/- 10% of the 50% target API ratio, the process temperature was set to 120 °C with +/- 10 °C disturbances, and a feed rate was held constant at 100 g/hr. After any API ratio change, adequate time was allowed to ensure steady state was reached before another change. Spectral data were collected at 20-s intervals during steady states and at different temperatures. The calibration sample set had 85 spectra at 40%, 45%, 47.5%, 50%, 52.5%, 55%, and 60% ratios.

Figure 2. (A) Absorption NIR spectra of API, polymer, and a 50/50 (w/w) extrudate in full scale. (B) Transflectance NIR spectra in common scale acquired during extrusion.

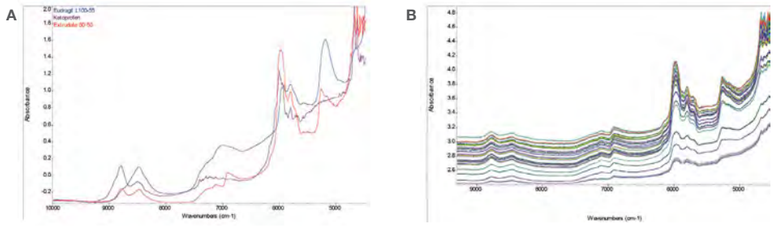

Figure 2A shows the overlaid NIR spectra of ketoprofen, Eudragit, and 50:50 (w/w) extrudate. Since ketoprofen and Eudragit are powders at room temperature, their spectra were measured using an integration sphere module of the Antaris II spectrometer. The extrudate spectrum was acquired with an NIR HME probe during an extrusion. All spectra have strong features in the first overtone C-H stretching region (~6000 cm^{-1}), and Eudragit and the extrudate have noticeable peak features in the first overtone O-H stretching region (~6900 cm^{-1}). **Figure 2B** shows the overlaid NIR spectra of calibration samples and a noticeable baseline up-drift, likely attributed to the scattering of air bubbles formed during the HME process and the variation in effective pathlength.

The Norris second derivative[10] was applied to the raw spectra to remove baseline drift, followed by a standard normal variant (SNV) to minimize the spectral pathlength variation. A PLS model[11] to estimate the ketoprofen concentration was then derived using the Thermo Scientific™ TQ Analyst™ software (mean-centered spectral data; 5500-6650 cm^{-1} spectral range; 73 spectra for calibration and 12 for validation; significant model factors determined by Leave-One-Out cross validation). The number of significant PLS factors represents independent variables that affect sample spectral responses (e.g., concentration, impurities, density, opaqueness, or color).

Figure 3. Calibration results of API measurement.

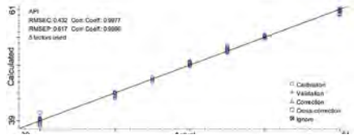

Figure 3 shows the PLS model with a 0.998 correlation coefficient, a 0.43% root mean squared error of calibration (RMSEC), and a 0.62% root mean squared error of prediction (RMSEP).

Figure 4. Overlay of the pre-blend profile and the API% trend based on the PLS model.

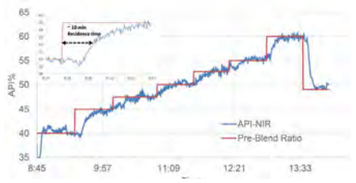

Figure 4 shows the calibration model applied to the HME process spectra, with the predicted API% tracking to the pre-blend profile. With a residence time of ~10 min, it takes 2-3 multiples of that (~20-30 min) to establish a new steady state after any ratio change.

Process stability monitoring with PCA

Continuous manufacturing requires controlling the production process in steady state to ensure smooth production and stable product quality. Traditionally, an HME process (with material flow rates, extrusion temperature, screw speed, and other variables) is considered at its steady state when operational parameters (e.g., torque, material temperature, and pressure) reach their equilibria. NIR spectra not only provide chemical information of the samples (blending ratio, API/binder interactions), but also are sensitive to the physical properties of the sample (color, temperature, density) and are, therefore, a more incisive, responsive, and comprehensive process indicator for product quality control. For a successful chemometrics model, extracting the relevant multivariate NIR spectral data is critical.

To simulate potential fluctuations during manufacturing, feed rate and temperature variables were introduced as process disturbances. Sample spectra were acquired at 20-s intervals, the raw data was processed with the 2nd derivative and SNV to remove spectral baseline drift and variations in spectral path length, and the PCA calculation was made across a 9150 to 4710 cm^{-1} region.

Figure 5. Process temperature robustness study: (A) temperature impact on NIR spectra; and (B) prediction of API% with a +/- 10 °C temperature variation.

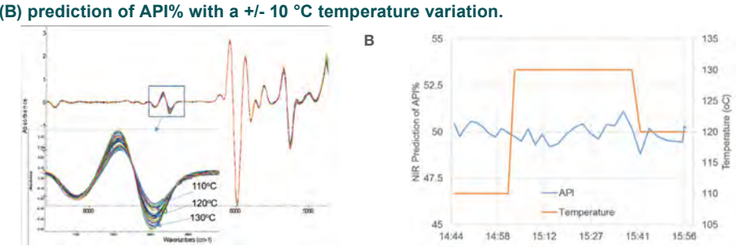

Figure 5A shows the 2nd derivative NIR spectra of samples collected at 3 temperatures with prominent spectral changes (at ~6900 cm^{-1}), likely due to the increased H-O bonding at elevated temperatures. In the PLS model, this spectral region was purposely excluded to reflect the API concentration change, minimizing interference from temperature-induced variation (5500-6650 cm^{-1} correlation range).

Figure 5B shows the API% change with temperature ramping from 110 to 130 °C to simulate variation in a real HME process, while maintaining the 50% pre-blend API ratio and feed rate of 100 g/hr. The predicted API% hovers at ~49-51%. These results suggest that the developed PLS model for API% prediction is robust within the +/- 10 °C temperature variation.

Figure 6. PC score plot of (A) temperature response and (B) feed rate response.

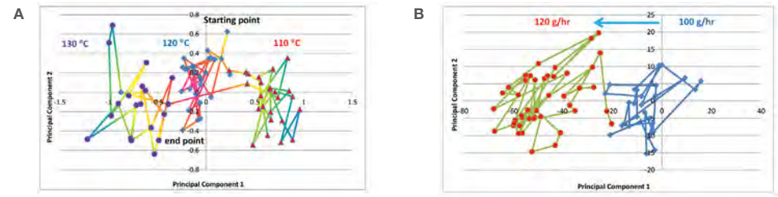

Figure 6A is a PC score plot of the temperatures response experiment that started with a process temperature of 120 °C and maintained a feed rate of 100 g/hr. The sample spectra formed a tight cluster of PC points (middle) in the PC domain. After the process stabilized, a 10 °C decrease was introduced. Spectral response changed accordingly: the resulting PC data point moved away from that cluster after about 6 sampling times (~ 2 min) to a form a new cluster locus. Similar PC point movement was observed for the temperature change (110-130 °C). The distance between two clusters represents a property shift in the hot melt. **Figure 6B** is a PC score plot of the feed rate response experiment. The temperature was maintained at 120 °C. The process started with a 100 g/hr material feed rate. Once it was stabilized, the feed rate was increased to 120 g/hr.

***Note:** *The API concentrations for the temperature and feed rate experiments are different; hence, the PC1 / PC2 ranges are different in the plots.*

PCA defines its principal component (PC) domain space through an iteration of information extraction from a calibration sample set, and converts each sample spectrum consisting of thousands of data points into a reduced (e.g., 2D or 3D) data point in a PC domain. The number of dimensions in a PC domain relates to the number of affecting variables (e.g., concentration, degree of cross-link, sample color, density), with the first several PCs covering the majority of the spectral information. Scores, or coefficients, of PCs are projections of a measured sample spectrum in a PC domain. By converting a spectrum into a PC point, responses during an HME process can be shown in a 2D or 3D trend plot. Because NIR spectra directly measure the extrudate, the trajectory of PC coordinates better represents an HME process state, offers insight into the process dynamics, and allows development of a more comprehensive control strategy.

CONCLUSIONS

Continuous manufacturing requires in-process monitoring of critical process parameters to ensure product consistency, like FT-NIR coupled with chemometrics modelling for in-line HME monitoring used here. A PLS model was successfully developed for API concentration prediction by carefully selecting the relevant NIR spectral region and was proven robust with a +/- 10 °C fluctuation. A PCA-based model was also developed to monitor the process state shift in response to disturbances in temperature and feed rate. Because the NIR spectrum is a direct measurement of the extrudate product, the trajectory of the PC movement offers insight to the process dynamics. Moreover, the PCA method relies solely on an accumulation of multiple batches of good process spectral data to define the steady state, does not require a calibration model, is independent of the product formulation, and is easy to implement. Finally, because NIR is nondestructive and fast, an NIR-based quality monitoring methodology can be easily transferred from process development to manufacturing.

REFERENCES

1. Schaber S.D., Gerogiorgis D.I., et al. Ind. Eng. Chem. Res., 2011, 50:17, 10083-10092.
2. Thiry J., Krier F., Evrard B. Int. Pharmaceut., 2015, 479:1, 227-240.
3. Breitenbach J. Eur. J. Pharm. Biopharm., 2002, 54:2, 107-117.
4. Crowley M.M., Zhang F., et al. Drug Dev. Ind. Pharm., 2007, 33:9, 909-926.
5. FDA Guidance for Industry. PAT – a framework for innovative pharmaceutical development, manufacturing, and quality assurance. Rockville, MD: Food and Drug Administration, 2004.
6. ICH Q8(R2), Pharmaceutical Development, Part I: Pharmaceutical development, and Part II: Annex to pharmaceutical development, 2009.
7. Markl D., Wahl P.R., et al. AAPS PharmSciTech, 2013, 14:3, 1034-44.
8. MacPhail N., Meyer R.F, et al. Spectroscopy Special Issues, 2011, 26:8.
9. Abdi H. and Williams L.J., Wires. Comput. Stat., 2010, 2, 433-459.
10. Rinnan A., van den Berg F., Engelsen S.B. Trends Anal. Chem., 2009, 28:10, 1201-1222.
11. Geladi P. and Kowalski B.R., Anal. Chim. Acta, 1986, 185, 1-17.

TRADEMARKS & LICENSING

ThermoFisher SCIENTIFIC

RETURN TO 'CONTENTS' PAGE

Using Raman spectroscopy and SEM to gain insights to API dispersion in hot melt extrusion

Antonis Nanakoudis[1], Mohammed Ibrahim[2], and Rui Chen[2], Thermo Fisher Scientific, Eindhoven, The Netherlands[1] and Madison, WI, USA[2]

ABSTRACT

An investigation of acetaminophen solid dispersions prepared by hot melt extrusion (HME) using Raman imaging and scanning electron microscopy (SEM) was performed, showing that a high screw speed favors the formation of a desirable amorphous dispersion. While Raman imaging provides a molecular-level depiction of the solid physical states of these extrudates by allowing the distribution of multiple chemical species to be visualized, SEM excels in spatial resolution to monitor the HME particle size reduction, especially in the sub-µm scale. Together, Raman and SEM provide holistic insight into the HME process.

Phenom XL Desktop SEM (left) and Thermo Scientific DXR3xi Raman Imaging Microscope (right)

INTRODUCTION

The pharmaceutical industry uses hot melt extrusion to prepare solid dispersions of poorly soluble active pharmaceutical ingredients (APIs) and for creating controlled-release medications.[1] The APIs are compounded with a thermoplastic polymer matrix, which acts as a solid solvent for the drug molecules, and extruded to form a solid dispersion. An amorphous API dispersion is desirable from a solubility perspective (no lattice energy to overcome prior to dissolution) and from a post-manufacturing standpoint (reduces the risk of aggregation or physical change).

Various analytical techniques have been used to characterize the physicochemical factors of hot melt extrudates relevant to HME process design and optimization.[2–5] We previously reported on the use of Terahertz (THz) Raman imaging to characterize the solid physical states of acetaminophen (APAP) in a hydroxypropyl methylcellulose (HPMC) matrix prepared by HME.[6] While Raman imaging can distinguish between crystalline and amorphous APAP and map the APAP distribution in HPMC, the spatial resolution of this visualization is limited at ~1 µm. Scanning electron microscopy offers a higher spatial resolution (nm scale) than optical techniques. SEM yields images with a characteristic three-dimensional appearance that has been used to probe the surface morphology of extrudates, especially the crystalline structure. By correlating molecular-level interactions and solid physical state changes with morphological variations, the Raman/SEM combination provides a holistic insight into the multifaceted HME process.

Here we used THz Raman imaging and SEM to investigate the solid physical states of APAP in HPMC matrix prepared by HME to analyze and compare extrudates from two different HME processes at different screw speeds, to assess the impact on formation of solid dispersions.

METHODS

Materials

Acetaminophen (APAP; Spectrum Chemicals, Gardena, CA), a crystalline BCS I drug with a melting point of 169°–170°C, was chosen as the model API. Hydroxypropyl methylcellulose (HPMC; Ashland, Wilmington, DE) E5 was used as the polymer matrix.

Hot melt extrusion

An 11-mm twin-screw extruder, Thermo Scientific Process 11 (Thermo Fisher Scientific, Karlsruhe, Germany), was used for the HME processes (screw profile design and process configuration shown in Figure 1). Zone 1 was the feeding zone. Zones 2 through 8 were mixing, conveying, and discharge zones. Zone 9 is a die that reduces barrel configuration to a single circular 5-mm diameter orifice.

Figure 1. The Thermo Scientific Process 11 Twin Screw Extruder configuration.

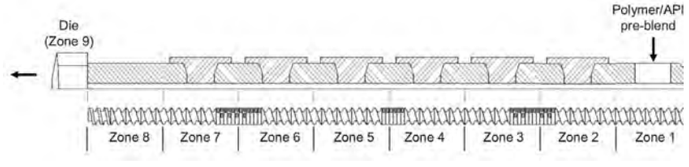

Table 1. HME processes, parameters, and zones analyzed.

HME Process	Extrusion Temp. (°C)	Screw Speed (rpm)	Feeder Screw Speed (rpm)	Zones Analyzed
H	170	200	24	Z3, Z7
L	170	50	6	Z3, Z7

The blending ratio of APAP and HPMC was 30:70 (w/w). Two HME processes were performed at different screw speeds (Table 1), withdrawing small amounts of samples when the extrusion reached the steady state. Samples were then pressed into thin films using a hydraulic press with heating panels at 40 °C to be analyzed by Raman imaging and SEM.

Raman imaging

Raman imaging was performed on a DXR3xi Raman Imaging Microscope (532 nm laser, 8 mW power at the sample), with data acquisition and processing by Thermo Scientific OMNICxi Software. Raman images were obtained by the Correlation Profiling option, using the THz region (≤ 200 cm^{-1}) of the crystalline APAP Raman spectrum as a reference. The profile shows the correlation between the spectrum at each pixel (sampling point) in the Raman image and the specified reference spectrum. The rainbow-colored intensity scale represents the degree of correlation to the reference spectrum by color, and a greater similarity produces a higher intensity value. A value of 1.0 (in red) indicates that the sample and reference spectra are identical. For direct comparison, a correlation range of 0.75-1 was applied to all the Raman images.

SEM imaging

All SEM images were acquired using a Phenom XL Desktop SEM equipped with a CeB6 source, and a Phenom Pharos Desktop SEM equipped with an FEG source. SEM images were acquired with a solid-state back-scattered electron detector (BSD), sensitive to atomic number variations. Due to the non-conductive nature of extrudates, the low-vacuum setting of 60 Pa was used for all experiments to avoid charging artefacts. Settings for acceleration voltage (10 kV) and spot size (medium value) allowed high-resolution imaging with a sufficient signal-to-noise ratio.

RESULTS AND DISCUSSION

Figure 2. a: Raman spectra from the blue, green and red regions. b-c: Raman images (100x objective; 0.5 µm pixel size) of the samples from Zone 3 extruded at 50 rpm or 200 rpm. d-e: SEM images of the same samples (3000x magnification).

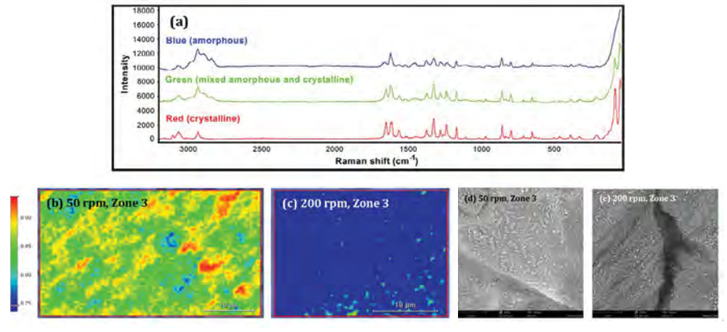

2a shows the representative Raman spectra of amorphous (blue), partially-amorphous (green), and crystalline APAP (red). There is a strong, sharp peak at 89 cm^{-1} unique to crystalline APAP that can be ascribed to the crystalline lattice vibrations (phonon mode). The spectra of the amorphous region and the partially-amorphous region contain contributions from the polymeric matrix. 2b-c show the Raman images of Zone 3 samples from Process H (high 200-rpm screw speed) and L (low 50-rpm screw speed). At the lower speed (Process L, 2b), the sample contains primarily partially-amorphous dispersion (green) and crystalline APAP (red). In contrast, at the higher speed (Process H, 2c) the sample consists of predominantly amorphous dispersion (blue). SEM corroborates these observations (2d-e). The Process L sample (2d) exhibits appreciable amount of well-defined, rectangular crystal structures (crystalline APAP) and some smaller, irregular bulk shaped particles (partially-amorphous solid dispersion) ranging from sub-µm to 15 µm. Alternately, the Process H sample (2e), exhibits more irregular shaped particles (partially-amorphous solid dispersion) ranging from sub-µm to ~2 µm.

Figure 3. a-b: Raman images (100× objective; 0.5 µm pixel size) of the samples from Zones 3 and 7 extruded at 200 rpm. c-d: SEM images of the same samples 3000x magnification).

3a-b show Raman images of the samples from two different zones of Process H (200 rpm). At the early stage (Zone 3, 3a), the APAP was present as partially-amorphous (green) and amorphous (blue) solid dispersions. The late stage sample (Zone 7, 3b) exhibits near-uniform, amorphous solid dispersions (blue). This is consistent with the SEM (3c-d). The Zone 3 sample (3c) shows large amount of irregular bulk shaped partially-amorphous solid dispersions, whereas the Zone 7 sample (3d) exhibits uniform and homogeneously mixed mass with wrinkled surface, indicating a near-complete amorphous dispersion.

Figure 4. SEM images (a-b: 3000x magnification) and (c-d: 7000x magnification) of the samples from Zones 3 and 7 extruded at 50 rpm.

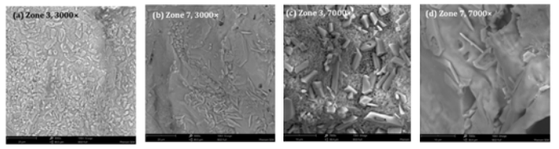

Figure 4 shows the SEM images of the samples from different zones of Process L (50 rpm). Zone 3 sample (4a) shows morphological characteristics of both crystalline APAP and partially-amorphous solid dispersion. Zone 7 (4b) shows a largely smooth surface (amorphous solid dispersion) with pockets of well-defined crystalline APAP and partially-amorphous solid dispersion morphological features. These samples were also examined using a higher magnification of 7000× (Figure 4c-d). Zone 3 extrudate (4c) has a rough, porous surface comprised of spherical texture, suggesting its partially-amorphous nature. The crystals on top appear to be smooth-surfaced rectangles and polyhedrons. Zone 7 extrudate (4d) displays a porous, dense underlying surface with both defined crystal structures and irregular shaped particles partially embedded into the surface. The coexistence of crystalline APAP, partially-amorphous solid dispersion and amorphous dispersion towards the final stage of this HME process suggests a highly inefficient extrusion process.

CONCLUSIONS

Our investigation of acetaminophen solid dispersions prepared by HME using Raman imaging and SEM compared extrudates from two different HME processes of different screw speeds. At the early stage, low screw speed resulted in partially amorphous dispersion and crystalline APAP but high screw speed led to predominantly amorphous and partially-amorphous dispersion. At the late stage, high screw speed exhibited a uniform, homogeneously mixed surface indicative of a near-complete amorphous dispersion but low screw speed displayed a dense surface with pockets of crystalline APAP and partially amorphous APAP dispersions. Raman imaging and SEM analyses confirm that a high screw speed favors the formation of amorphous APAP solid dispersion. While Raman imaging provides molecular-level insight to the underlying chemistry of an HME process by allowing the distribution of multiple chemical species to be visualized, SEM excels in spatial resolution to monitor the particle size, especially in the sub-µm scale, critical for understanding the solid physical state transformation of the API in HME.

REFERENCES

1. M.A. Repka, S. Bandari, et al., *Int. J. Pharm.* **535**, 68–85 (2018).
2. R. Censi, M.R. Gigliobianco, et al., *Pharmaceutics* **10**, 89 (2018).
3. S. Baghel, H. Cathcart, and N.J. O'Reilly, *J. Pharm. Sci.* **105**, 2527-2544 (2016).
4. P. Hitzer, T. Bäuerle, et al., *Anal. Bioanal. Chem.* **409**, 4321–4333 (2017).
5. N. Furuyama, S. Hasegawa, et al., *Int. J. Pharm.* **361**, 12–18 (2008).
6. M. Ibrahim, J. Zhang, et al., *AAPS PharmSciTech* **20**, 62 (2019).

TRADEMARKS/LICENSING

ThermoFisher SCIENTIFIC

RETURN TO 'CONTENTS' PAGE

Quality control and validation

Using Raman spectroscopy and SEM to gain insights to API dispersion in hot melt extrusion

Antonis Nanakoudis[1], Mohammed Ibrahim[2], and Rui Chen[2], Thermo Fisher Scientific, Eindhoven, The Netherlands[1] and Madison, WI, USA[2]

ABSTRACT

An investigation of acetaminophen solid dispersions prepared by hot melt extrusion (HME) using Raman imaging and scanning electron microscopy (SEM) was performed, showing that a high screw speed favors the formation of a desirable amorphous dispersion. While Raman imaging provides a molecular-level depiction of the solid physical states of these extrudates by allowing the distribution of multiple chemical species to be visualized, SEM excels in spatial resolution to monitor the HME particle size reduction, especially in the sub-µm scale. Together, Raman and SEM provide holistic insight into the HME process.

Phenom XL Desktop SEM (left) and Thermo Scientific DXR3xi Raman Imaging Microscope (right)

INTRODUCTION

The pharmaceutical industry uses hot melt extrusion to prepare solid dispersions of poorly soluble active pharmaceutical ingredients (APIs) and for creating controlled-release medications.[1] The APIs are compounded with a thermoplastic polymer matrix, which acts as a solid solvent for the drug molecules, and extruded to form a solid dispersion. An amorphous API dispersion is desirable from a solubility perspective (no lattice energy to overcome prior to dissolution) and from a post-manufacturing standpoint (reduces the risk of aggregation or physical change).

Various analytical techniques have been used to characterize the physicochemical factors of hot melt extrudates relevant to HME process design and optimization.[2–5] We previously reported on the use of Terahertz (THz) Raman imaging to characterize the solid physical states of acetaminophen (APAP) in a hydroxypropyl methylcellulose (HPMC) matrix prepared by HME.[6] While Raman imaging can distinguish between crystalline and amorphous APAP and map the APAP distribution in HPMC, the spatial resolution of this visualization is limited at ~1 µm. Scanning electron microscopy offers a higher spatial resolution (nm scale) than optical techniques. SEM yields images with a characteristic three-dimensional appearance that has been used to probe the surface morphology of extrudates, especially the crystalline structure. By correlating molecular-level interactions and solid physical state changes with morphological variations, the Raman/SEM combination provides a holistic insight into the multifaceted HME process.

Here we used THz Raman imaging and SEM to investigate the solid physical states of APAP in HPMC matrix prepared by HME to analyze and compare extrudates from two different HME processes at different screw speeds, to assess the impact on formation of solid dispersions.

METHODS

Materials

Acetaminophen (APAP; Spectrum Chemicals, Gardena, CA), a crystalline BCS I drug with a melting point of 169°–170°C, was chosen as the model API. Hydroxypropyl methylcellulose (HPMC; Ashland, Wilmington, DE) E5 was used as the polymer matrix.

Hot melt extrusion

An 11-mm twin-screw extruder, Thermo Scientific Process 11 (Thermo Fisher Scientific, Karlsruhe, Germany), was used for the HME processes (screw profile design and process configuration shown in Figure 1). Zone 1 was the feeding zone. Zones 2 through 8 were mixing, conveying, and discharge zones. Zone 9 is a die that reduces barrel configuration to a single circular 5-mm diameter orifice.

Figure 1. The Thermo Scientific Process 11 Twin Screw Extruder configuration.

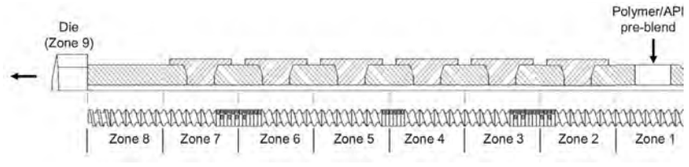

Table 1. HME processes, parameters, and zones analyzed.

HME Process	Extrusion Temp. (°C)	Screw Speed (rpm)	Feeder Screw Speed (rpm)	Zones Analyzed
H	170	200	24	Z3, Z7
L	170	50	6	Z3, Z7

The blending ratio of APAP and HPMC was 30:70 (w/w). Two HME processes were performed at different screw speeds (Table 1), withdrawing small amounts of samples when the extrusion reached the steady state. Samples were then pressed into thin films using a hydraulic press with heating panels at 40 °C to be analyzed by Raman imaging and SEM.

Raman imaging

Raman imaging was performed on a DXR3xi Raman Imaging Microscope (532 nm laser, 8 mW power at the sample), with data acquisition and processing by Thermo Scientific OMNICxi Software. Raman images were obtained by the Correlation Profiling option, using the THz region (≤ 200 cm^{-1}) of the crystalline APAP Raman spectrum as a reference. The profile shows the correlation between the spectrum at each pixel (sampling point) in the Raman image and the specified reference spectrum. The rainbow-colored intensity scale represents the degree of correlation to the reference spectrum by color, and a greater similarity produces a higher intensity value. A value of 1.0 (in red) indicates that the sample and reference spectra are identical. For direct comparison, a correlation range of 0.75-1 was applied to all the Raman images.

SEM imaging

All SEM images were acquired using a Phenom XL Desktop SEM equipped with a CeB6 source, and a Phenom Pharos Desktop SEM equipped with an FEG source. SEM images were acquired with a solid-state back-scattered electron detector (BSD), sensitive to atomic number variations. Due to the non-conductive nature of extrudates, the low-vacuum setting of 60 Pa was used for all experiments to avoid charging artefacts. Settings for acceleration voltage (10 kV) and spot size (medium value) allowed high-resolution imaging with a sufficient signal-to-noise ratio.

RESULTS AND DISCUSSION

Figure 2. a: Raman spectra from the blue, green and red regions. b-c: Raman images (100x objective; 0.5 µm pixel size) of the samples from Zone 3 extruded at 50 rpm or 200 rpm. d-e: SEM images of the same samples (3000x magnification).

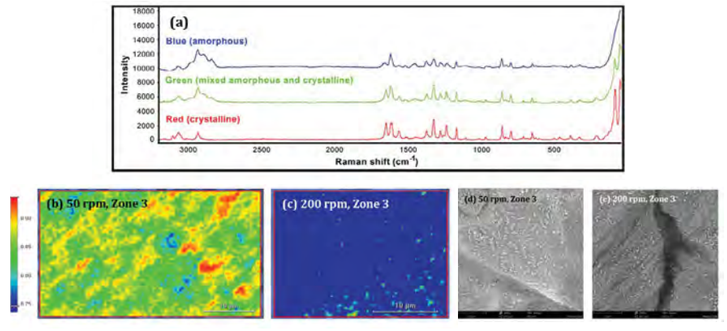

2a shows the representative Raman spectra of amorphous (blue), partially-amorphous (green), and crystalline APAP (red). There is a strong, sharp peak at 89 cm^{-1} unique to crystalline APAP that can be ascribed to the crystalline lattice vibrations (phonon mode). The spectra of the amorphous region and the partially-amorphous region contain contributions from the polymeric matrix. 2b-c show the Raman images of Zone 3 samples from Process H (high 200-rpm screw speed) and L (low 50-rpm screw speed). At the lower speed (Process L, 2b), the sample contains primarily partially-amorphous dispersion (green) and crystalline APAP (red). In contrast, at the higher speed (Process H, 2c) the sample consists of predominantly amorphous dispersion (blue). SEM corroborates these observations (2d-e). The Process L sample (2d) exhibits appreciable amount of well-defined, rectangular crystal structures (crystalline APAP) and some smaller, irregular bulk shaped particles (partially-amorphous solid dispersion) ranging from sub-µm to 15 µm. Alternately, the Process H sample (2e), exhibits more irregular shaped particles (partially-amorphous solid dispersion) ranging from sub-µm to ~2 µm.

Figure 3. a-b: Raman images (100× objective; 0.5 µm pixel size) of the samples from Zones 3 and 7 extruded at 200 rpm. c-d: SEM images of the same samples 3000x magnification).

3a-b show Raman images of the samples from two different zones of Process H (200 rpm). At the early stage (Zone 3, 3a), the APAP was present as partially-amorphous (green) and amorphous (blue) solid dispersions. The late stage sample (Zone 7, 3b) exhibits near-uniform, amorphous solid dispersions (blue). This is consistent with the SEM (3c-d). The Zone 3 sample (3c) shows large amount of irregular bulk shaped partially-amorphous solid dispersions, whereas the Zone 7 sample (3d) exhibits uniform and homogeneously mixed mass with wrinkled surface, indicating a near-complete amorphous dispersion.

Figure 4. SEM images (a-b: 3000x magnification) and (c-d: 7000x magnification) of the samples from Zones 3 and 7 extruded at 50 rpm.

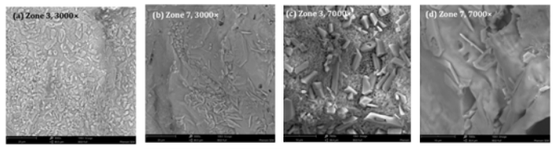

Figure 4 shows the SEM images of the samples from different zones of Process L (50 rpm). Zone 3 sample (4a) shows morphological characteristics of both crystalline APAP and partially-amorphous solid dispersion. Zone 7 (4b) shows a largely smooth surface (amorphous solid dispersion) with pockets of well-defined crystalline APAP and partially-amorphous solid dispersion morphological features. These samples were also examined using a higher magnification of 7000× (Figure 4c-d). Zone 3 extrudate (4c) has a rough, porous surface comprised of spherical texture, suggesting its partially-amorphous nature. The crystals on top appear to be smooth-surfaced rectangles and polyhedrons. Zone 7 extrudate (4d) displays a porous, dense underlying surface with both defined crystal structures and irregular shaped particles partially embedded into the surface. The coexistence of crystalline APAP, partially-amorphous solid dispersion and amorphous dispersion towards the final stage of this HME process suggests a highly inefficient extrusion process.

CONCLUSIONS

Our investigation of acetaminophen solid dispersions prepared by HME using Raman imaging and SEM compared extrudates from two different HME processes of different screw speeds. At the early stage, low screw speed resulted in partially amorphous dispersion and crystalline APAP but high screw speed led to predominantly amorphous and partially-amorphous dispersion. At the late stage, high screw speed exhibited a uniform, homogeneously mixed surface indicative of a near-complete amorphous dispersion but low screw speed displayed a dense surface with pockets of crystalline APAP and partially amorphous APAP dispersions. Raman imaging and SEM analyses confirm that a high screw speed favors the formation of amorphous APAP solid dispersion. While Raman imaging provides molecular-level insight to the underlying chemistry of an HME process by allowing the distribution of multiple chemical species to be visualized, SEM excels in spatial resolution to monitor the particle size, especially in the sub-µm scale, critical for understanding the solid physical state transformation of the API in HME.

REFERENCES

1. M.A. Repka, S. Bandari, et al., *Int. J. Pharm.* **535**, 68–85 (2018).
2. R. Censi, M.R. Gigliobianco, et al., *Pharmaceutics* **10**, 89 (2018).
3. S. Baghel, H. Cathcart, and N.J. O'Reilly, *J. Pharm. Sci.* **105**, 2527-2544 (2016).
4. P. Hitzer, T. Bäuerle, et al., *Anal. Bioanal. Chem.* **409**, 4321–4333 (2017).
5. N. Furuyama, S. Hasegawa, et al., *Int. J. Pharm.* **361**, 12–18 (2008).
6. M. Ibrahim, J. Zhang, et al., *AAPS PharmSciTech* **20**, 62 (2019).

ThermoFisher SCIENTIFIC

RETURN TO 'CONTENTS' PAGE

Ensure accurate analysis with innovative software solutions

Steve Lowry and Katherine Paulsen – Thermo Fisher Scientific, 5225 Verona Road, Madison, WI 53711 USA

ABSTRACT

FTIR offers the capacity to reveal the composition of solids, liquids, and gases. By determining the similarity between a sample spectrum and that of a reference, this technique enables the identification of unknown materials, the confirmation of incoming or outgoing production materials, and the relative purity of the sample. Here we examine how advanced software can enhance spectral comparison, incorporate reproducible workflow, and generate reports for a variety of needs.

Thermo Scientific™ Nicolet™ Summit FTIR spectrometer with touchscreen and OMNIC™ Paradigm™ Software

INTRODUCTION

One of the most popular applications of FTIR spectroscopy is mathematically comparing the spectrum from one sample to that of a known, good reference material. The process of comparing two spectra is used as a verification technique for incoming materials, evidence in a court of law, and even proof that a patented chemical is unique. The most simple and reliable metric for measuring the similarity between infrared spectra is determining the correlation value. A perfect correlation results in a value of 100 and any small differences between the two spectra reduces the value. Even with modern FTIR spectrometers, it is extremely rare to have a perfect correlation of 100. Most labs consider a correlation value of 95 or better to indicate a strong spectral match. In a typical industrial environment, the goal is to verify that the sample falls within an acceptable level of purity relative to the good reference material.

DISCUSSION

Using the QCheck function to compare spectra

The Thermo Scientific™ OMNIC™ Paradigm Software is instrument control software used to collect spectral and other data, analyze samples, and create workflows, making it easy to automate analyses. In the software, a function called QCheck makes it easy to compare one spectrum to one or more reference spectra. In this example, we use QCheck to verify that a plastic sample is actually the specified material, polystyrene. In OMNIC Paradigm Software, we overlaid the spectra from the polystyrene reference material and our plastic sample. Visually, the two spectra look similar, with peak locations and intensities that overlap well (Figure 1). The QCheck function mathematically calculates the correlation of these two spectra and displays the QCheck analysis in a report with a high correlation value of 99.81 (Figure 2).

Figure 1. Sample spectrum and best match from QCheck analysis.

Figure 2. An example QCheck analysis report.

The QCheck analysis offers a fast and reliable method that allows optimization of the algorithm to fit needs, such as selecting the best spectral region for the application, determining how much signal averaging is required to produce an acceptable spectrum, and deciding on a Pass/Fail correlation value. Figure 3 shows the different variables that can be optimized in the QCheck function, the most popular of which is selecting specific regions to conduct the correlation comparison.

Using a QCheck workflow

The OMNIC Paradigm Software makes it easy to analyze single samples, as shown above. QC laboratories will often document those steps in a Standard Operating Procedure to ensure that multiple samples can be analyzed consistently. The OMNIC Paradigm Software also includes a

Figure 3. The setup screen for the QCheck analysis.

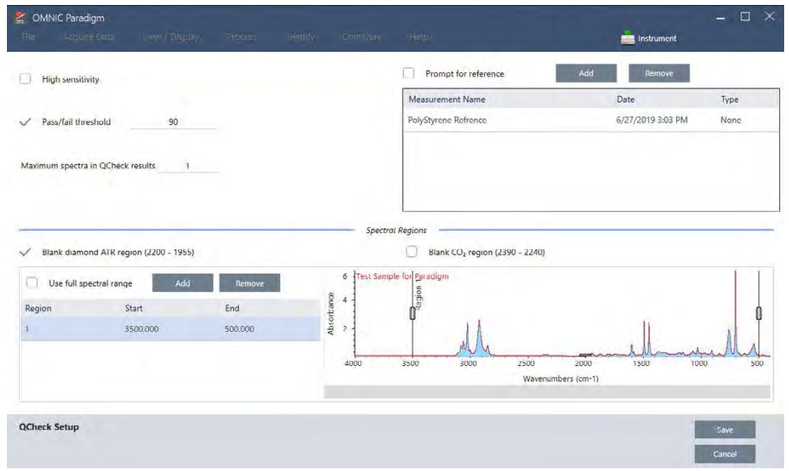

feature set called workflows to automate those steps for busy laboratories that need consistent answers (Figure 4).

Figure 4. Workflow template and a list of possible functions.

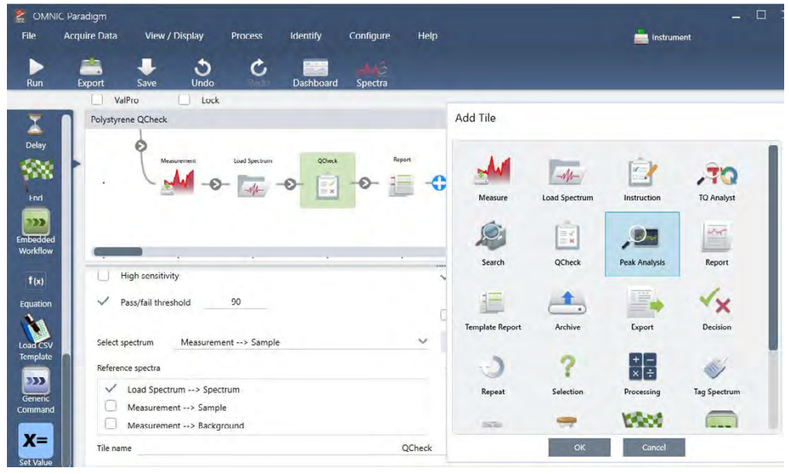

Once the basic workflow is created, it is easy to manipulate the workflow to run multiple samples and save the results in a file that can be opened in Microsoft Excel. If more than one sample needs to be analyzed, a repeat loop can be inserted to measure multiple samples in a row. Figure 5 shows an example with a Repeat tile added to replicate the workflow 20 times. To save time, this workflow collects a single background spectrum to use with all the other measurements. An Export Tile was appended to the save results to a text file. If needed, an Exit tile could be added to exit the workflow to run fewer than 20 samples.

Simplifying workflow development with OMNIC Paradigm Software

Workflows are created by simply dragging and dropping the tiles around on the touchscreen from the left sidebar into the center canvas area, double-clicking a tile to edit the parameters, and clicking the Play button to get results (Figure 6). With eighteen tiles available and the ability to customize

Figure 5. A schematic overview of the final workflow. The workflow, spectra, results, and reports are all automatically saved.

instructional prompts with text and images, there are endless possibilities for streamlining any method or SOP. After collecting a sample, processing a spectrum, and establishing a history, users can even click the "Create Workflow" button to automate a customized workflow. Spectra can be displayed while the instrument is scanning or hidden from the user, and will be automatically archived to a user-selected location.

Figure 6. An example OMNIC Paradigm workflow. This sample workflow displays a starting instructional prompt, followed by steps to measure the background, measure the sample, generate the report, and archive the results, with the associated screens that will display.

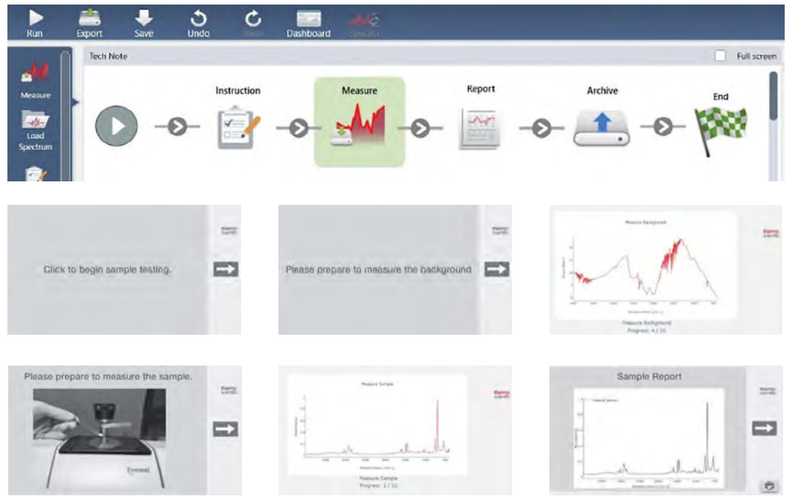

CONCLUSIONS

OMNIC Paradigm is a modern FTIR spectroscopy platform that enables a mathematical comparison between one spectrum and another to assess sample purity. By automating the process further, OMNIC Paradigm helps automatically create workflows based on the spectral processing history, and saves the information to a powerful database to retrieve later or perform further analysis.

TRADEMARKS/LICENSING

ThermoFisher SCIENTIFIC

RETURN TO 'CONTENTS' PAGE

Security and compliance simplified: the Nicolet Summit FTIR Spectrometer and OMNIC Paradigm Software

Matthew Gundlach and Katherine Paulsen – Thermo Fisher Scientific, 5225 Verona Road, Madison, WI 53711 USA

ABSTRACT

With the sheer number and scope of regulatory requirements faced by producers of pharmaceuticals and medical devices, the extra burden of commissioning new systems and keeping them in compliance can put a strain on internal resources. They're not the only group affected: consumer product, food and beverage, and manufacturing industries all need to monitor quality and safety across their processes. Regardless of the quality standards or regulations requiring compliance, the cost of poor quality can be high in terms of rejected lots, loss of purchasing contracts or worse, legal action. By coupling a secure system with a comprehensive tool set composed of FDA-compliant 21 CFR Part 11[1] tools, audit trails, qualification packages, certification services, and operator training designed to help navigate the regulatory environment, making measurements that are subject to regulations or performing work that requires verification of system performance becomes a less cumbersome, seamless part of the process.

Thermo Scientific™ Nicolet™ Summit FTIR spectrometer

INTRODUCTION

Ensuring that your data is safe and secure doesn't have to be daunting. A fully secured system, like the Thermo Scientific™ Nicolet™ Summit FTIR spectrometer, consists of three software applications: Security Administration, Audit Manager, and Thermo Scientific™ OMNIC™ Paradigm Software (Figure 1). Together the Audit Manager and Security Administration applications are also known as the Thermo Scientific Security Suite. Audit Manager logs events into the database and provides detailed event information and tracking. Security Administration controls access and system policies for each user. Secure tagging, a new feature that allows CROs and CMOs to give data access to users based on a secure tag, can be different for every piece of data. Finally, the instrument control software (OMNIC Paradigm) manages data collection, sample analysis, and workflow creation, and stores all spectral data in a relational database.

Figure 1. Security suite and instrument control.

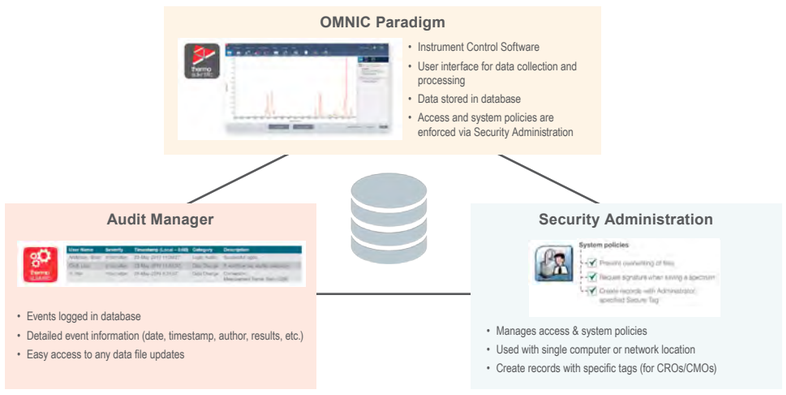

The **Security Administration** software gives lab managers the ability to control who has access to what data, can enable or disable certain commands and features within the instrument software, and can require scientists or technicians to digitally sign their data to comply with 21 CFR Part 11 regulations. For larger labs, this software can manage multiple instruments from a single installation (i.e., distributed configuration).

The **Audit Manager** software captures system event information (when a user logged on, when a spectrum was collected, when data was saved, etc.) and provides easy filtering tools to quickly find events by date, user name, computer ID, and more. Audit Manager includes additional event details like specific spectral processing information, which provides a single location for an auditor to review. All audit trail information is stored in an SQL or user-specific database.

The **Thermo Scientific OMNIC Paradigm** instrument control software is used to collect data (spectral data; metadata about the author, processing history, tags, and results; audit trail information), analyze samples, and create workflows. Like Audit Manager, OMNIC Paradigm Software stores all spectral data in a database, which provides more data storage flexibility and security. Users can even assign tags to measurements to make querying their data easy. OMNIC Paradigm Software uses MariaDB® relational database by default, but users can define the database of their choice from a supported list (Table 1).

Table 1. Relational databases compatible with OMNIC Software.

Database	Supported Versions
Aurora DB	MySQL 5.6 MySQL 5.7
MariaDB*	10.0 10.1 10.2 10.3
Oracle	11g Release 2 12c Release 1 12c Release 2 18c
SQL Server	2012 2014 2016 2017

*The Maria DB is the default database.

DISCUSSION

The benefits of a database

Storing data in a database provides several benefits for users and auditors. Databases are designed to organize and retrieve large data sets and filter them by time, author, and instrument name. Databases also allow metadata to be automatically linked to the spectral data, which greatly strengthens the audit trail. In the software, the audit trail not only shows that a spectrum has changed, but also shows exactly what changes were made to the spectrum in the details field. Finally, databases ensure files are always in sync, which means no duplicates or orphans can exist.

A Remote Database option for OMNIC Paradigm software allows users to configure the database to reside on the instrument or in another location, like on a company server that is already equipped with a set of security measures to control data integrity (Figure 2). Only a user who has the appropriate permission given by the administrator can access that remote data. Further, multiple instruments can be connected to a single remote database, enabling the ability to review the data of several systems from one location.

Figure 2. The Remote Database option

Customer server with MariaDB, SQL, or Oracle database

Taking advantage of compliance services

It is important to have documented evidence to show that the hardware and software have been installed correctly and are functioning as intended. Having access to trained service engineers who can provide Installation Qualification/Operational Qualification (IQ/OQ) services during the installation of a new instrument, after moving an instrument to another location, or at any other time you might request, is an essential cog in the process. Our instrument validation and qualification services are offered through Unity Lab Services at **unitylabservices.com/compliance**.

Compliance documentation

IQ documents verify that the system has arrived and is installed correctly, ensuring that all the parts are included, the instrument has arrived undamaged, everything is connected properly, and that the environment is suitable for the instrument. OQ documents verify the system functions as intended, such that the hardware and software are working well together and spectral data are being accurately collected. Our team also documents that Security Suite software is installed correctly, security policies are being verified, and event logging is being performed.

Performing system qualification checks

Operating in a regulated environment requires you to make sure your instrument is performing as expected, usually once per day. Conducting this performance check is referred to as "System Qualification", and should be performed by the most common methods referred to in the European, US, Japanese, and Chinese Pharmacopeias. The OMNIC Paradigm Software includes automated analysis procedures that make sure your spectrometer is compliant with the performance requirements outlined in the Pharmacopeia documents (Figure 3). Each instrument includes its own traceable internal polystyrene standard, so testing your instrument performance is as easy as clicking a button.

Figure 3. Example qualification workflow on the Nicolet FTIR

CONCLUSIONS

No matter what you make or do, ensuring regulatory compliance places an extra burden on internal resources. Integrating a database with advanced software capabilities for instrument control and audit management capabilities places the more onerous tasks on the computer resources. Choosing a fully secured system, like the Nicolet Summit FTIR spectrometer with the Thermo Scientific Security Suite and OMNIC™ Paradigm Software pre-installed eases the burden while capturing the data needed to ensure compliance.

NOTE

1.21CFR Part 11 tools: Software tools and expertise to configure systems for complete compliance with FDA requirements for data security and traceability. "Persons who use closed systems to create, modify, maintain, or transmit electronic records shall employ procedures and controls designed to ensure the authenticity, integrity, and…confidentiality of electronic records …Such procedures and controls shall include: Validation of systems to ensure consistent intended performance, Protection of records to enable their accurate and ready retrieval, Limiting system access to authorized individuals"

TRADEMARKS/LICENSING

ThermoFisher SCIENTIFIC

RETURN TO 'CONTENTS' PAGE

Instrument Resolution – Measurement and Effect on Performance in UV-Visible Spectrophotometry

Daniel A. Frasco, Ph.D., Thermo Fisher Scientific, Madison, WI, 53711 USA

ABSTRACT

When defining the method parameters for a UV-Visible spectrophotometer, one essential question that must be asked is "What bandwidth should be used?" This poster explains the reasons why bandwidth is important, its relation to the resolving power of the instrument, and how the resolving power of an instrument is checked.

INTRODUCTION

To achieve the optimum performance from a UV-Visible spectrophotometer (in terms of absorbance and wavelength accuracy) it is necessary to consider the resolution of the monochromator. In its most basic definition, resolution is the ability of an instrument to separate light into finite, distinct wavelength regions and distinguish these finite regions from each other (i.e., its ability to separate two adjacent peaks). When a monochromator is set to a nominal wavelength, an approximately triangular intensity distribution of wavelengths emerges (Figure 1). The monochromator wavelength is set to λ_2, but in fact wavelengths ranging from λ_1 to λ_3 leave the exit slit. The total spread of wavelengths $\lambda_1 - \lambda_3$ is termed the spectral slit width (SSW). The width of the profile at half-peak height is termed the effective spectral slit width (ESW), and this is equivalent to the bandwidth of the instrument.

Figure 1. Definition of bandwidth

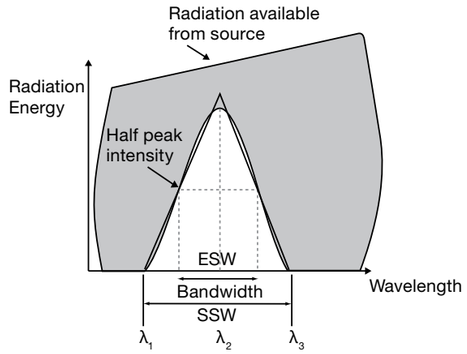

Resolution is primarily governed by the physical slit width of the instrument, in combination with the dispersion within the system. Reducing the physical slit width decreases the bandwidth. Decreasing the bandwidth (effective spectral slit width) improves the ability of the instrument to resolve closely spaced peaks.

When variable bandwidth is available, it might seem best to use the smallest available bandwidth at all times. However, reducing the bandwidth leads to a reduction in energy through the system, which means a corresponding decrease in the signal-to-noise ratio. Therefore, it is not possible to have both the highest possible resolution and the lowest possible noise level at the same time. It is necessary to make a compromise between the need to resolve the spectral features of the sample being scanned and the requirement to keep the noise down to an acceptable level.

The maximum bandwidth you can use without causing unacceptable degradation of the spectrum depends on the width of the peaks that you need to resolve. The natural bandwidth of a peak is defined as the width of the peak at half the height (compare to the ESW definition, see Figure 1) when measured at infinite resolution. As a general rule, the error in peak measurement will be negligible if the effective spectral slit width (ESW) does not exceed 10% of the Natural Bandwidth of the peak.[1]

METHODS

Use of lamp emission spectrum

A lamp emission spectrum that has intense lines covering the UV and visible range can be used to verify the bandwidth accuracy of an instrument. Example lamps with fundamental lines that can be used for evaluation include mercury and deuterium. In this example the deuterium lamp emission profile of the 656.1 nm line was measured at 0.5, 1.0, and 1.5 nm bandwidths. The apparent width of the band at half-peak height is taken to be the effective spectral slit width (ESW) of the instrument.

Figure 2. Deuterium lamp emission line profiles

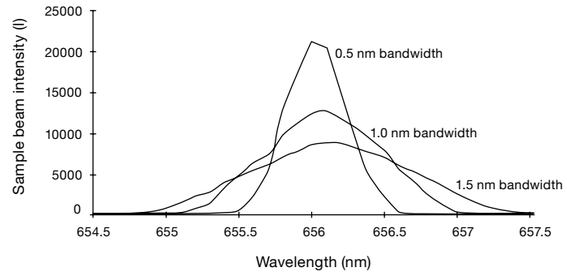

Use of benzene vapor spectrum

The benzene vapor absorption spectrum, which serves as a reference standard, has a minor peak at 259.6 nm that can be resolved from the main band if the instrument has a ESW of less than 0.5 nm. A stoppered cell containing benzene vapor was scanned, and the calculations shown in Figure 3 were performed). To demonstrate the resolving capacity of the spectrophotometer, the ratio value (R) calculated using the ratio between the absorbance maximum and minimum of the standard should be greater than 0.1. The effects of increasing the bandwidth are shown in Figure 4.

Figure 3. Resolution calculation using benzene vapor spectrum

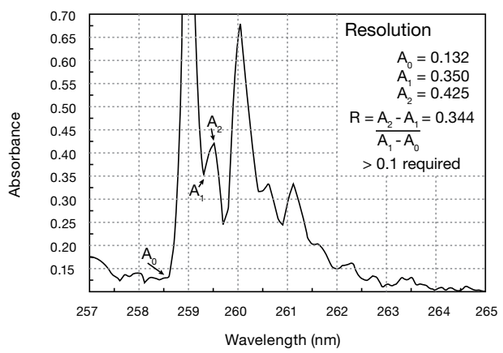

Use of toluene in hexane solution spectrum

A 0.020% v/v solution of toluene in hexane is the most widely used reference standard to demonstrate the resolution using a known peak to trough ratio by recording the spectrum (Figure 5). The acceptance criteria for the ratio of the absorbance at the maximum at 269 nm to that at the minimum at 266 nm will depend on the specification of the instrument and any potential regulatory guidelines including pharmaceutical performance verification requirements.

Figure 4. Effect of increasing bandwidth on the benzene vapor spectrum

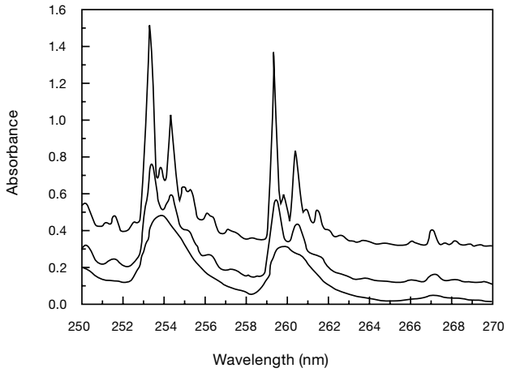

Figure 5. Effect of bandwidth on toluene in hexane solution

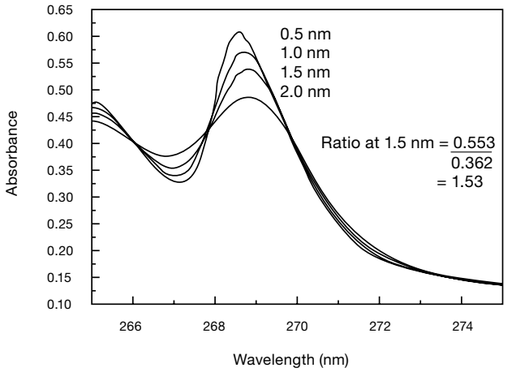

CONCLUSIONS

Determining the ideal spectral bandwidth for each method is essential to generate the highest quality data. The optimal slit width for spectral analysis is not necessarily 1.0 nm, and while a narrower spectral bandwidth can improve resolution of adjacent peaks, it comes with a decrease in the signal-to-noise ratio. Therefore, choosing the spectral bandwidth should depend on the analysis needs. There are multiple ways to evaluate the spectral bandwidth of an instrument using various reference standards to ensure it will have adequate resolving power for the intended application.

REFERENCES

1. C. Burgess and T. Frost, "Standards and Best Practice in Absorption Spectrometry" (Blackwell Science, Oxford, 1999).

TRADEMARKS/LICENSING

ThermoFisher SCIENTIFIC

RETURN TO 'CONTENTS' PAGE

Benefits of transmission mode in XRD

G. Schmidt[1], S.Welzmiller[2], R.Yerly[3], C.Fontugne, H.Pillière, E.Berthier, Thermo Fisher Scientific, [1] Waltham, MA, United States, [2] Ecublens, Switzerland, [3] Artenay, France

CONTEXT & OBJECTIVES

Powder X-ray diffraction (XRD) is an analytical technique which offers a wide range of instrumental configuration, in order to respond to specific structural characterization. The most frequent setup is based on the irradiation of the sample surface by an incident beam, to allow the sample surface emission of the diffracted signal (Bragg-Brentano or asymmetric geometry). However, diffraction signal can also be obtained by transmission, as described by the Debye-Scherrer geometry. Because of its original instrumental configuration, ARL EQUINOX X-Ray diffractometers allow to perform both setups and to get complementary information on the sample itself.

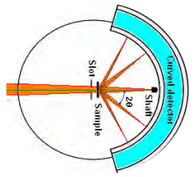

METHODS

XRD investigation of Ibuprofen in transmission mode

ARL EQUINOX 100
Benchtop X-Ray diffractometer

Powder sample holder in transmission configuration

- Many generic products of the Ibuprofen on the market
- Additionally to talc, using additives to accomplish different requirements (Sodium Citrate and Calcium Carbonate to minimize the harm to the stomach & Sucrose for a more pleasant taste)

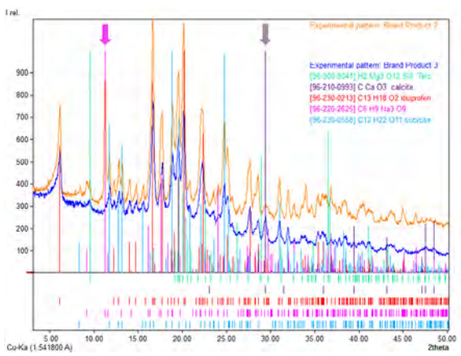

In contrast to Product 3, Product 2 contains Sodium Citrate (purple) but no Calcite (grey) (arrows mark differences). The presence of Sucrose (blue) is confirmed.

Copper radiation

- Good resolution of the ARL EQUINOX 100 in transmission mode
- Qualitative phase analysis & trace phases detection in only 10 min.
- Ability to clearly resolve the crystalline phases in different pharmaceutical mixtures

► ARL EQUINOX 100 : easy-to-use tool for all fields of pharmaceutical research or production from preformulation through to QA/QC of the final drug product

Data comparison with a Cu & Mo radiation

Co catalysis sample conditioned in a cup transmission

Possibility of symmetric acquisition in +/- 60°2θ, ARL EQUINOX 5000

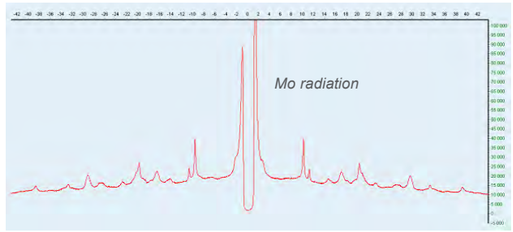

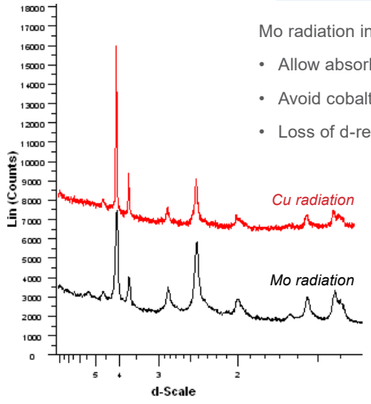

Mo radiation in transmission, benefits and consequences

- Allow absorbing components analysis
- Avoid cobalt secondary fluorescence
- Loss of d-resolution

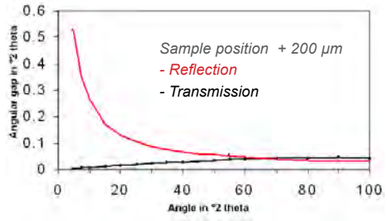

More space making easier in situ analysis

Free from sample positioning problems

- Positioning advantages

Phase transition on an organic sample

ARL EQUINOX 3000 with a parabolic mirror for fast acquisition

Sample conditioned in a capillary (1mm diameter)

Capillary sample holder for transmission analysis

Capillary set on a goniometer head and aligned by camera on ex-situ device

Acquisition every 10° up to 70°C and then every 5° in cooling

Acquisition time : 3 min.

A novel approach for the analysis of single grains

Gandolfi stage

Analysis of single crystal or small volume samples (~ 1mm[3]) without the need of a dedicated single crystal XRD system

ARL EQUINOX 3000 / 5000
Powder X-Ray diffractometers

- Rotation of the sample according to three-circle
- Fast analysis of single crystal or small volume samples not suitable for conventional XRD systems
- Possible analysis from phase identification to ab initio structure solution with proper software applications

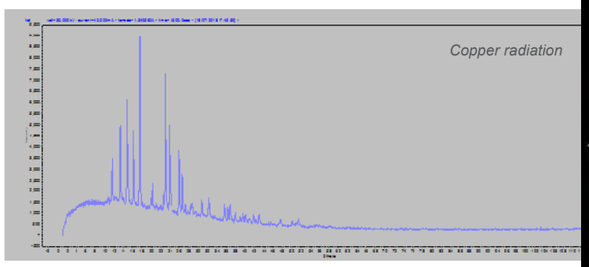

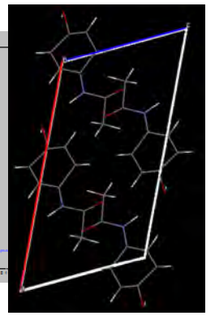

- Extracted intensities from a one-hour data set
- Ab initio structure solved thanks to various software solutions (FOX, EXPO2014, GSAS-II, etc.) and refined using Rietveld methods

NOTES
1.Corresponding author: eric.berthier@thermofisher.com
2.Keywords: Diffraction, X-Ray, Capillary, Gandolfi, Dynamic studies, ARL EQUINOX

TRADEMARKS/LICENSING

ThermoFisher SCIENTIFIC

RETURN TO 'CONTENTS' PAGE

Nucleic acid quantification and qualification

The Acclaro basics of detecting and monitoring contaminants in nucleic acid samples

Sean Loughrey and Brian Matlock, Thermo Fisher Scientific, Wilmington, DE, USA

ABSTRACT

The Thermo Scientific™ NanoDrop™ One microvolume UV-Vis spectrophotometer enables accurate quantification of nucleic acid or protein samples in the presence of common contaminants. The novel Thermo Scientific™ Acclaro™ Sample Intelligence technology allows the NanoDrop One instrument to provide more information about sample quality by identifying common contaminants and delivering true sample concentrations. This information enables more informed decisions for downstream experiments and provides information for troubleshooting problematic extractions. Here we describe how the Acclaro Contaminant Identification (ID) feature detects protein contamination in nucleic acid samples.

INTRODUCTION

*Here, in the first of a series of four posters, we show the basics of how the Acclaro Contaminant ID feature can accurately identify contaminants by subtracting the contribution of the contaminant from the original absorbance value to deliver an accurate nucleic acid concentration and to minimize the effects that contaminants in purified nucleic acid samples have on downstream workflows. In companion posters, we address overcoming calculation errors attributable to protein, reagent (phenol, guanidine, and others), or nucleic acid contaminants.**

The quantification of nucleic acids has traditionally been performed by absorbance measurements at 260 nm, a simple method of choice in the molecular biology laboratory to obtain concentration and purity information about nucleic acid samples. A consideration when evaluating samples is that many contaminants from the nucleic acid extraction process also absorb in various regions of the UV spectrum (Figure 1). When the contaminant absorption is in the same UV range as nucleic acids, it can directly affect the quantification result by 1) artificially inflating the A260 value, which results in an inaccurate concentration, and 2) affecting the purity ratios, which have long been a method to assess the presence of UV-absorbing contaminants. Relying on purity ratios alone does not provide a complete assessment of the potential contaminants in nucleic acid samples. However, using purity ratios with full-spectral data can enhance the ability to determine nucleic acid sample purity and ensure a more accurate concentration from an A260 measurement.

Figure 1. Contaminants can affect the UV absorbance spectrum of a nucleic acid preparation. The UV absorbance spectrum of a) a pure nucleic acid sample (with a peak at 260 nm and a trough at 230 nm), b) a nucleic acid sample contaminated with guanidine, and c) a nucleic acid sample contaminated with phenol.

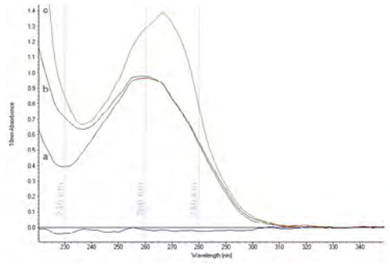

Table 1. Generally accepted purity ratio ranges for "pure" nucleic acid samples in TE buffer.

Samples	260/280	260/230
DNA	1.8–2.0	1.8–2.2
RNA	2.0–2.2	1.8–2.2

In general, verification that purity ratios fall into an acceptable range (Table 1) for a "pure" nucleic acid sample is sufficient. However, when purity ratios fall outside the accepted range, a visual analysis of the sample spectrum or technical assistance may become necessary. Until now, analysis of a sample's spectrum has been purely qualitative, and identification of specific contaminants has relied on the experience of the researcher.

The Acclaro sample intelligence technology built into the NanoDrop One spectrophotometer provides a quantitative method for contaminant identification in a sample by using a chemometric approach to compare the sample spectrum against a reference library of spectra and make predictions about the presence and identity of contaminants. The Acclaro contaminant ID feature can detect protein, phenol, and guanidine salts in dsDNA and RNA samples.

The software alerts users to the presence of a contaminant in real time, displaying a yellow contaminant ID icon (⚠, Figure 2 Measurement screen, left) next to the sample number. Tapping on this icon reveals full contaminant analysis details (Figure 2 Containment Analysis screen, right) that include deconvolved spectra, identified contaminants, corrected DNA concentration, and a %CV (representing the confidence of the prediction). In this poster, we share how the Acclaro sample intelligence technology detects protein contamination in nucleic acid samples.

*This poster is part of a series of 4 posters that highlight how to manage various contaminants in nucleic acid samples using NanoDrop spectrophotometers and Acclaro software Contaminant ID:

- The Acclaro basics of detecting and monitoring contaminants in nucleic acid samples
- Overcoming concentration calculation errors in the presence of phenol, guanidine, and other reagents
- Overcoming concentration calculation errors in the presence of proteins
- Overcoming concentration calculation errors in the presence of nucleic acid contamination

Figure 2. Acclaro Contaminant ID. *Measurement screen* (left) displays the Acclaro Contaminant ID icon when the Acclaro algorithms have detected a contaminant in this dsDNA sample. 3b) *Contaminant Analysis screen* (right) shows the absorbance spectra of the Original (DNA plus contaminant), Corrected (DNA minus contaminant, with the characteristic peak at 260 nm and trough at 230 nm), and Impurity (identified contaminant, with the characteristic peak at 280 nm and an increase in absorbance below 250 nm) and includes data on concentration, 260/280 and 260/230 ratios. To ensure reproducible results, the Corrected value should be used in planning downstream experiments.

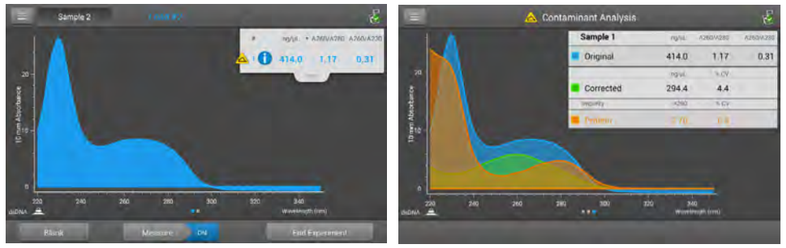

Contaminants in nucleic acid samples

One significant contaminant in nucleic acid preparations that contributes to the absorbance at 260 is protein, inflating the concentration of the nucleic acid, and is usually detected by a decrease in the 260/280 purity ratio. The decrease in this ratio occurs because the amino acid residues (tryptophan, tyrosine, and phenylalanine) and the cystine disulfide bonds in protein absorb at 280 nm. While the 260/280 ratio was originally a sensitive detection method for DNA contamination in protein preparations (Warburg, 1942)[1] and was later adopted by the molecular biology community to detect protein contamination in nucleic acid preparations, it has limitations. Because the extinction coefficients of proteins are very small relative to those of nucleic acids, it takes a large amount of protein to affect the 260/280 purity ratio (Glasel, 1995, Huberman, 1995, and Manchester, 1995).[2-4] Nonetheless, scientists do see nucleic acid preparations with low 260/280 purity ratios.

Another significant contaminant in purified nucleic acids is phenol, which historically has been used to separate protein from nucleic acids since the 1950s. Although various protocols and formulations have been developed over the years, the most popular technique was developed in the 1980s, using a mixture of guanidinium thiocyanate, phenol, and chloroform that allowed scientists to obtain highly pure, undegraded total RNA in a single step (Chomczynski and Sacchi, 1987, Chomczynski and Sacchi, 2006)1-2. This served as the development model for many RNA extraction kits using different formulations of phenol, guanidium thiocyanate, and chloroform to lyse cells and denature proteins including DNases and RNases. Calculating and assessing a purity ratio (using absorbances at 260/280 or 260/230) is the traditional method to detect phenol contamination. However, this method is not very effective because phenol has an absorbance peak at 270 nm and the purity ratios of pure phenol are close to the ratios observed for pure DNA and RNA (Table 1).

MATERIALS AND METHODS

Double-stranded DNA (dsDNA) stock was prepared by diluting a salmon sperm DNA solution (Invitrogen™, #15632-011) in Tris-EDTA (TE) buffer (Fisher BioReagents™, pH 7.6, BP-2474-500). A protein stock was prepared by diluting a solution of bovine serum albumin (BSA, Sigma Aldrich®, #A7284) in TE buffer. The stock concentrations were determined on the NanoDrop One spectrophotometer against a TE blank. Mass calculations were made using the factor 50 ng-cm/µL for dsDNA and the extinction coefficient E1% 6.7 for BSA.

Five replicates for each of nine mixtures of DNA and protein were then prepared to generate the mixtures shown and measured on the NanoDrop One spectrophotometer against a TE blank, using a fresh 1.5 µL aliquot of the appropriate mixture for each replicate. The software-calculated concentrations (corrected and original/uncorrected) and Acclaro Contaminant identity data were then used to generate the data sets presented (Table 2).

The original (uncorrected) concentrations versus the software-corrected concentrations were compared, and results are discussed below. Since mixtures 1–4 did not contain protein levels high enough to trigger an Acclaro Contaminant ID result, the corrected DNA concentration for mixtures 1 through 4 were determined by performing the Acclaro spectral analysis using the Thermo Scientific™ TQ Analyst™ software package.

Table 1. DNA and protein mixtures analyzed with the NanoDrop One instrument. Uncorrected DNA concentration was determined using the dsDNA application and corrected values for mixtures 5–9 were obtained directly from NanoDrop One Acclaro contaminant analysis results. The contaminant ID icon (⚠) denotes mixtures having protein contamination levels high enough to trigger an Acclaro result.

Mixture	1	2	3	4	5	6	7	8	9
% DNA (by mass)	100.0	57.1	40.0	28.6	16.7	10.0	7.1	4.8	1.6
% Protein (by mass)	0.0	42.9	60.0	71.4	83.3	90.0	92.9	95.2	98.4
Uncorrected DNA [conc] ng/µL	531.8	534.7	542.1	571.5	591.3	644.4	672.9	740.4	1097.6
Corrected DNA [conc] ng/µL	526.8	523.9	525.9	540.4	541.1	554.6	549.2	547.3	560.1
260/280 Purity Ratio	1.94	1.89	1.84	1.74	1.60	1.45	1.34	1.21	0.89
260/230 Purity Ratio	2.45	1.67	1.34	0.90	0.61	0.41	0.32	0.26	0.19
Acclaro Flag	No	No	No	No	⚠	⚠	⚠	⚠	⚠

RESULTS AND DISCUSSION

Table 2 presents a summary of the data provided in more detail in the companion poster titled "Overcoming Concentration Calculation Errors in the Presence of Proteins", with Acclaro Contaminant ID data obtained for nine mixtures containing DNA and different levels of contamination (protein in this example). As the contamination level increases, the discrepancy between the corrected and the original (uncorrected) results becomes larger, emphasizing how protein contamination can inflate an A260 concentration result. The software-corrected results show how the algorithm can quantitatively correct for these levels of protein contamination and provide a more accurate DNA concentration than the A260 value alone. A large amount of protein contamination is required before a significant change in the 260/280 purity ratios is observed: only after the protein contaminant level increases above 72% by weight does the 260/280 ratio drop significantly. At high levels of contamination, Acclaro software flags the sample and displays a corrected concentration, which are within 10% of the result for the DNA only control. Although mixture 9, with the highest amount of protein contamination where its protein contamination represents >98% of the analyte mass in the sample, shows the largest difference between the corrected and uncorrected concentration results, the software-corrected value brings its result within 10% of the actual DNA concentration. The Acclaro Contaminant ID feature of the NanoDrop One spectrophotometer delivers a definitive advantage for nucleic acid samples by providing a corrected DNA concentration and identifying contaminants present.

CONCLUSIONS

Experiments that use nucleic acids require that the concentration and purity of the sample is known. The UV-Vis method used for the quantification of nucleic acid preparations relies on the absorbance of nucleic acid molecules at 260 nm to determine the concentration of nucleic acids in solution. Contaminants that are co-purified with nucleic acids can also absorb light in the UV region of the spectrum, which leads to overestimating the calculated nucleic acid concentration. Traditionally, purity ratios have been relied upon as an indication of the presence of contaminants in nucleic acid samples. "Out of range" purity ratios can indicate the presence of contaminants but cannot provide information on the identity and amount of the contaminant present. The Acclaro sample intelligence technology in the NanoDrop One spectrophotometer provides a chemometric approach for contaminant identification using UV spectrum analysis. This feature empowers researchers to 1) identify the type of contaminant present in their sample 2) determine the level of contamination and 3) obtain a corrected nucleic acid concentration. By using the Acclaro sample intelligence technology, you can make informed decisions on how to troubleshoot sample preparations to reduce contamination and how to proceed using a sample in downstream experiments.

REFERENCES

1. Warburg, O. and W. Christian. 1942. Isolation and crystallization of Enolase. *Z. Biochem.* 1942. 310:384-421.
2. Glasel, J.A. 1995. Validity of nucleic acid purities monitored by 260 nm/280 nm absorbance ratios. *Biotechniques* 18:62–63.
3. Huberman, J.A. 1995. Importance of measuring nucleic acid absorbance at 240 nm as well as at 260 nm and 280 nm. *Biotechniques* 18:636.
4. Manchester, K.L. 1995. Value of A260/A280 Ratios for the Measurement of Purity of Nucleic Acids. *Biotechniques* 19:208-210.

TRADEMARKS/LICENSING

ThermoFisher SCIENTIFIC

RETURN TO 'CONTENTS' PAGE

Overcoming concentration calculation errors in the presence of phenol, guanidine, and other reagents

Sean Loughrey and Brian Matlock, Thermo Fisher Scientific, Wilmington, DE, USA

ABSTRACT

The new Thermo Scientific™ Acclaro™ Sample Intelligence technology built into the Thermo Scientific™ NanoDrop™ One microvolume UV-Vis spectrophotometers allows scientists to accurately quantify their nucleic acid samples in the presence of common contaminants carried over from nucleic acid extraction methods. In this study, we measured the concentration of DNA in the presence of various amounts of phenol contamination. We then compared the uncorrected versus the software-corrected concentration values. The results showed that the corrected DNA concentrations were within 10% of the concentration of the DNA-only control, demonstrating the effectiveness of the software algorithm to identify phenol contamination, properly correct the DNA concentration values, and provide a more accurate concentration than from the A260 value alone. This information enables informed decision-making about sample use in downstream experiments and provides information for troubleshooting extractions.

Thermo Scientific™ NanoDrop™ One and One^{C} Microvolume UV-Vis spectrophotometers

INTRODUCTION

*Here, in the third of a series of four posters, we show the basics of how the Acclaro Contaminant ID feature can accurately identify phenol, guanidine, and other reagent contaminants by subtracting the contribution of the contaminant from the original absorbance value to deliver an accurate nucleic acid concentration and to minimize the effects that reagent components in purified nucleic acid samples have on downstream workflows. In companion posters, we address the basics of the Acclaro Contaminant ID feature and overcoming calculation errors attributable to protein or other contaminants.**

Quantification of nucleic acids remains an essential technique in experimental biological and biomedical techniques and workflows involving nucleic acid samples. Techniques such as PCR, qPCR, next-generation sequencing, and cloning requiring determinations of sample purity and other variables can affect nucleic acid samples and their use in downstream experiments. Sample concentration, purity, and quality are the main sample variables that can be obtained by various instruments.

The quantification of nucleic acids has traditionally involved absorbance measurements at 260 nm. An important consideration for this method is that contaminants from the nucleic acid extraction process absorb in various regions of the UV spectrum, which can directly affect the accuracy of the quantification result.

Reviewing purity ratios, by verifying that the ratios fall into an acceptable range (Table 1), has been the primary method used to assess the presence of UV-absorbing contaminants. However, relying on purity ratios alone does not provide a complete assessment of potential contaminants. Combining purity ratios with full-spectral data greatly enhances the ability to determine not only the purity of a nucleic acid sample, but also an accurate concentration via A260 absorbance. Until now, analysis of a sample spectrum was a qualitative endeavor that relied heavily on a researcher's experience and ability to identify specific contaminants from it.

Table 1. Purity ratio ranges generally accepted for pure nucleic acid samples in TE buffer. Notice that the purity ratio for pure phenol does not deviate greatly from the purity ratios for pure nucleic acids.

Samples	260/280	260/230
DNA	1.8–2.0	1.8–2.2
RNA	2.0–2.2	1.8–2.2
Pure Phenol	1.6	2

The Acclaro technology in the NanoDrop One spectrophotometer provides a cutting-edge quantitative approach for contaminant identification by using chemometric analysis of the chemical components present and helps scientists make informed decisions about using samples in downstream reactions and workflows that may be labor intensive or expensive or consume rare samples. The Acclaro contaminant ID feature can detect contaminants in dsDNA and RNA samples and provides software alerts to indicate the presence of a contaminant in real time, displaying a yellow contaminant ID icon (⚠) next to the sample number that can expand to show full contaminant analysis details (deconvolved spectra, identified contaminants, corrected DNA concentration, and a %CV representing the confidence of the prediction), all described in more detail in "The Acclaro basics of detecting and monitoring contaminants in nucleic acid samples". Here we present data obtained by the Acclaro Contaminant ID feature and show how this technology can accurately detect phenol contamination in nucleic acid samples and provide accurate DNA concentration values.

Phenol contamination in nucleic acid samples

The use of phenol to separate protein from nucleic acids has a history dating back to the 1950s. Although various protocols and formulations have been developed over the years, the most popular technique was developed in the 1980s, using a mixture of guanidinium thiocyanate, phenol, and chloroform that allowed scientists to obtain highly pure, undegraded total RNA in a single step[1-2].This served as the development model for various RNA extraction kits, including TRIzol™ kit (Thermo Fisher Scientific), TRI Reagent® kit (Molecular Research Center, Inc), QIAzol® kit (Qiagen), TriPure™ kit (Sigma-Aldrich), TRISure™ kit (Bioline), and RNAzol® kit (Molecular Research Center). These kits use different formulations of phenol, guanidium thiocyanate, and chloroform to lyse cells and denature proteins including DNases and RNases. However, traces of these reagents found in purified nucleic acid samples may affect downstream workflows.

*This poster is part of a series of 4 posters that highlight how to manage various contaminants in nucleic acid samples using NanoDrop spectrophotometers and Acclaro software Contaminant ID:

- The Acclaro basics of detecting and monitoring contaminants in nucleic acid samples
- Overcoming concentration calculation errors in the presence of phenol, guanidine, and other reagents
- Overcoming concentration calculation errors in the presence of proteins
- Overcoming concentration calculation errors in the presence of nucleic acid contamination

Table 2. The DNA concentration of each dsDNA and phenol stock mixture and the DNA-only control (mixture 1) were determined with the NanoDrop One spectrophotometer using the dsDNA application. The corrected DNA concentration for mixtures 3 through 9 was obtained directly from the Acclaro contaminant analysis screen. The contaminant ID icon (⚠) denotes mixtures that have levels of phenol contamination high enough to trigger an Acclaro result. **Mixtures 1 and 2 did not contain high enough concentrations of phenol to trigger an Acclaro result, therefore, the corrected DNA concentrations for these mixtures were determined by performing the Acclaro spectral analysis algorithm using the Thermo Scientific™ TQ Analyst™ software package.

Mixture	1	2	3	4	5	6	7	8	9
Phenol content (ppm)	0.00	18.75	37.50	75.00	150.00	300.00	600.00	1200.00	1600.00
Target DNA conc ng/µL	225.0	225.0	225.0	225.0	225.0	225.0	225.0	225.0	225.0
Original (Uncorrected) DNA conc ng/µL	245.75	253.50	264.34	284.75	318.35	387.55	523.59	851.29	1041.50
Corrected DNA conc ng/µL	240.56**	238.67**	240.61	243.26	244.38	242.51	245.26	265.96	265.45
Corrected DNA conc ng/µL Std dev	0.61	0.95	0.79	1.24	0.76	0.85	0.87	5.47	3.26
260/280 Purity Ratio	1.89	1.85	1.83	1.79	1.75	1.70	1.71	1.53	
260/230 Purity Ratio	2.43	2.38	2.32	2.27	2.19	2.11	2.08	1.89	0.19
Acclaro Flag	No	No	⚠	⚠	⚠	⚠	⚠	⚠	⚠

The extraction procedure (Figure 2) will create an organic phase and an aqueous phase. The pH of the extraction solution will dictate which nucleic acid species is extracted: an acidic solution favors extraction of RNA into the aqueous phase; an alkaline solution extracts both DNA and RNA into the aqueous phase. Partially denatured proteins congregate in the interphase. Separation of nucleic acids from the denatured protein requires removal of the aqueous phase without disturbing the interphase. To avoid contamination of the purified nucleic acid with protein, phenol, or guanidium, removal of the aqueous phase requires experience and precise technique[3-5], which can be difficult for those new to extraction.

Figure 2. Phase separation typically observed when performing a conventional phenol-based nucleic acid extraction. The photograph shows how difficult it is to see the phase separation.

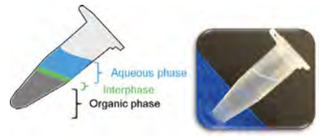

Phenol contamination can affect nucleic acid samples by effectively denature proteins, thus affecting downstream enzymatic steps, and with a high extinction coefficient at 270 nm, even low contamination can overestimate sample concentration.

Calculating and assessing a purity ratio (using absorbances at 260/280 or 260/230) is the traditional method to detect phenol contamination. However, this method is not very effective because phenol has an absorbance peak at 270 nm and the purity ratios of pure phenol are close to the ratios observed for pure DNA and RNA (Table 1). Later, we show how different amounts of phenol contamination affect the 260/280 or 260/230 purity ratios and nucleic acid quantification results and how the Acclaro Contaminant ID feature can accurately identify phenol contamination, by subtracting the contribution from phenol from the original absorbance value to deliver an accurate nucleic acid concentration.

MATERIALS AND METHODS

Stocks of DNA and phenol were prepared. A double stranded DNA (dsDNA) stock was prepared by diluting a salmon sperm DNA solution (Invitrogen, #15632-011) in Tris-EDTA (TE) buffer (Fisher BioReagents, pH 7.6, BP-2474-500). A phenol stock was prepared by diluting a buffer-saturated phenol (Fisher BioReagents, BP-1750) in TE buffer. The concentrations of the stocks were determined on the NanoDrop One spectrophotometer against a TE blank. Nine mixtures were prepared by adding various amounts of the DNA and phenol stocks (Table 2).

Five replicates for each of nine mixtures of DNA and protein were then prepared to generate the mixtures shown and measured on the NanoDrop One spectrophotometer against a TE blank. A fresh 1.5 µL aliquot of the appropriate mixture was used for each replicate. The software-calculated concentrations (corrected and original/uncorrected) and Acclaro Contaminant identity data were then used to generate the data sets presented (Table 1).

RESULTS AND DISCUSSION

Table 2 presents the Acclaro Contaminant ID data obtained for the nine mixtures. Note that the phenol component is expressed in parts per million (ppm), a conversion needed because its molar extinction coefficient is much larger than the extinction coefficient of dsDNA. For example, a 0.1% solution of phenol is 1,000 ppm. As the level of phenol increases from 37.5 ppm to 1,600 ppm, the discrepancy between the corrected and the uncorrected values increases. This clearly demonstrates how even tiny amounts of phenol contamination can inflate an A260 concentration result. The software-corrected results demonstrate the algorithm's effectiveness in identifying phenol contamination, properly correcting the concentration values, and providing a more accurate concentration result than the A260 value alone.

Figure 3 compares the uncorrected and the corrected DNA concentration data in the presence of different levels of phenol contamination. Note that the presence of phenol significantly inflates the concentration value. The Acclaro feature flags samples when phenol contamination is greater than ~18.75 ppm, thus illustrating the high sensitivity of the software at detecting phenol contamination. In all cases, the corrected DNA concentrations are within 10% of the concentration of the DNA-only control. Moreover, the concentration results were highly reproducible at high levels of phenol contamination, with average standard deviations under 5 ng/µL.

Figure 4 illustrates that increasing amounts of phenol contamination have a minor effect on both purity ratios. A DNA sample with a phenol contamination of 600 ppm has a 260/280 ratio of 1.71 and a 260/230 ratio of 2.08, values that are within the range of generally accepted values for pure nucleic acid samples. However, with this level of phenol contamination, the DNA concentration result is generally off by greater than two-fold. Our results support the importance of not relying solely on these ratios to assess the purity of a nucleic acid sample or detect contamination.

Figure 3. The DNA concentration after Acclaro correction is within 10% of the actual DNA concentration (DNA-only control) for all mixtures. Red bars represent the uncorrected DNA concentrations. The blue bars represent the corrected DNA concentrations reported by the Acclaro software (or as described in Material and Methods). The blue line is the average concentration for the phenol-free, DNA-only control (mixture 1: 245.75 ng/µL). The green dotted lines represent +/- 10% from the DNA-only control. Each data point represents the average of five measurements. Error bars represent one standard deviation from the mean.

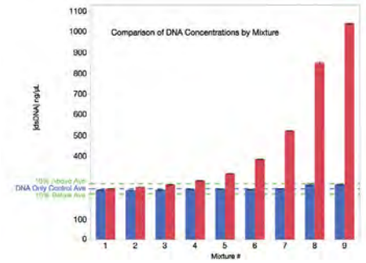

Figure 4. Average purity ratios were plotted for each dsDNA/phenol mixture. 260/230 purity ratio (red line); 260/280 purity ratio (blue line).

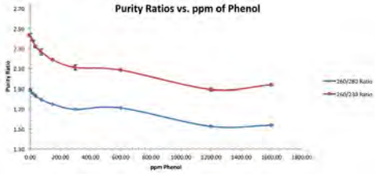

CONCLUSIONS

The trend toward complex and demanding high-throughput genomic workflows such as qPCR, next-generation sequencing, short tandem repeat (STR) analysis, and digital PCR require rigorous quality control checks for the input nucleic acid used in these workflows. These workflows require that the concentration and purity of the sample are known and pass quality control checks. UV measurements are commonly used to determine the concentration of nucleic acid samples prior to setting up genomic workflows. UV absorbance is quick and reliable, and the only quantification method that provides purity information (e.g., spectra, 260/280 and 260/230 absorbance ratios). Contaminants from nucleic acid extraction kits (e.g., phenol) absorb UV light in the same region of the UV spectrum as nucleic acids and their presence can lead to inflated nucleic acid concentration results. Traditionally, 260/280 and 260/230 ratios offer an indication of the presence of contaminants in nucleic acid solutions. Although purity ratios can indicate the presence of some contaminants, they do not provide definitive identity or amount of the contaminant. The Acclaro sample intelligence technology built into the NanoDrop One spectrophotometer provides a chemometric approach for contaminant identification using UV spectrum analysis. The Acclaro Contaminant ID feature accurately identifies phenol contamination present in nucleic acid samples, accurately calculates the amount of phenol contamination, and provides corrected nucleic acid concentration values that are more accurate than using absorbance at 260 nm alone.

REFERENCES

1. Chomczynski, P. and Sacchi, N. *Anal. Biochem.* 162: 156-159. 1987.
2. Chomczynski, P. and Sacchi, N. *Nature Protocols* Vol. 1 No.2: 581-585. 2006.
3. Oswald, N. *BiteSize Bio.* July 9th 2016. http://bitesizebio.com/384/the-basics-how-phenol-extraction-works
4. Plank, J. *BiteSize Bio.* May 3rd 2010. http://bitesizebio.com/3651/practical-application-of-phenolchloroform-extraction
5. Jankovic, J. *BiteSize Bio.* Nov. 23rd 2016. http://bitesizebio.com/31609/acid-phenol-chloroform-extraction

TRADEMARKS/LICENSING

ThermoFisher SCIENTIFIC

RETURN TO 'CONTENTS' PAGE

Overcoming concentration calculation errors in the presence of protein

Sean Loughrey and Brian Matlock, Thermo Fisher Scientific, Wilmington, DE, USA

ABSTRACT

The Thermo Scientific™ NanoDrop™ One microvolume UV-Vis spectrophotometer enables accurate quantification of nucleic acid or protein samples in the presence of common contaminants like protein. The novel Thermo Scientific™ Acclaro™ Sample Intelligence technology allows the NanoDrop One instrument to provide more information about sample quality by identifying common contaminants and delivering true sample concentrations. This information enables more informed decisions for downstream experiments and provides information for troubleshooting problematic extractions. Here we describe how the Acclaro Contaminant Identification (ID) feature detects protein contamination in nucleic acid samples.

INTRODUCTION

*Here, in the second of a series of four posters, we show the basics of how the Acclaro Contaminant ID feature can accurately identify protein contamination by subtracting the contribution of the contaminant from the original absorbance value to deliver an accurate nucleic acid concentration and to minimize the effects that protein components in purified nucleic acid samples have on downstream workflows. In companion posters, we address the basics of the Acclaro Contaminant ID feature and overcoming calculation errors attributable to reagent (phenol, guanidine, and others) or other contaminants.**

The quantification of nucleic acids has traditionally been performed by absorbance measurements at 260 nm, a simple method of choice in the molecular biology laboratory to obtain concentration and purity information about nucleic acid samples. A consideration when evaluating samples is that many contaminants from the nucleic acid extraction process also absorb in various regions of the UV spectrum (as shown in the first figure in the companion poster "The Acclaro basics of detecting and monitoring contaminants in nucleic acid samples"). The generally accepted purity ratio ranges for "pure" nucleic acid samples in TE buffer for DNA are 1.8–2.0 in the 260/280 ratio and 1.8–2.2 in the 260/230 ratio and for RNA are 2.0–2.2 for the 260/280 ratio and 1.8–2.2 for the 260/230 ratio. However, contaminant absorption in the same UV range as nucleic acids can directly affect the quantification result by artificially inflating the A260 value (resulting results in an inaccurate concentration) and by affecting the purity ratios that have long been a method to assess the presence of UV-absorbing contaminants. Relying on purity ratios alone cannot provide a complete assessment of the potential contaminants in nucleic acid samples, but using purity ratios with full-spectral data can enhance the ability to determine nucleic acid sample purity and ensure a more accurate concentration from an A260 measurement.

Figure 1. Pure DNA and pure protein spectra overlaid on the same graph. The DNA spectrum (green-blue) has the characteristic peak at 260 nm and trough at 230 nm, whereas, the protein spectrum (red-blue) has the characteristic peak at 280 nm and an increase in absorbance below 250 nm.

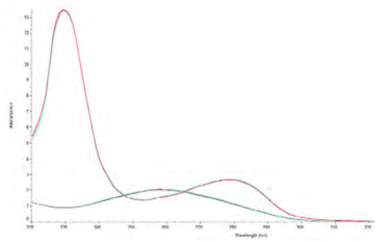

In general, verification that purity ratios fall into an acceptable range for a "pure" nucleic acid sample is sufficient. However, when purity ratios fall outside the accepted range, a visual analysis of the sample spectrum or technical assistance may become necessary. Until now, analysis of a sample's spectrum has been purely qualitative, and identification of specific contaminants has relied on the experience of the researcher.

The Acclaro sample intelligence technology built into the NanoDrop One spectrophotometer provides a quantitative method for contaminant identification in a sample by using a chemometric approach to analyze the chemical components present and algorithms to compare the sample spectrum against a reference library of spectra and make predictions about the presence and identity of contaminants. The Acclaro contaminant ID feature can detect contaminants in dsDNA and RNA samples and provides software alerts to indicate the presence of a contaminant in real time, displaying a yellow contaminant ID icon (⚠) next to the sample number that can expand to show full contaminant analysis details (deconvolved spectra, identified contaminants, corrected DNA concentration, and a %CV representing the confidence of the prediction), all described in more detail in "The Acclaro basics of detecting and monitoring contaminants in nucleic acid samples". In this poster, we share how the Acclaro sample intelligence technology detects protein contamination in nucleic acid samples.

*This poster is part of a series of 4 posters that highlight how to manage various contaminants in nucleic acid samples using NanoDrop spectrophotometers and Acclaro software Contaminant ID:

- The Acclaro basics of detecting and monitoring contaminants in nucleic acid samples
- Overcoming concentration calculation errors in the presence of phenol, guanidine, and other reagents
- Overcoming concentration calculation errors in the presence of proteins
- Overcoming concentration calculation errors in the presence of nucleic acid contamination

Table 1. DNA and protein mixtures analyzed with the NanoDrop One instrument. Uncorrected DNA concentration was determined using the dsDNA application and corrected values for mixtures 5–9 were obtained directly from NanoDrop One Acclaro contaminant analysis results. The contaminant ID icon (⚠) denotes mixtures having protein contamination levels high enough to trigger an Acclaro result.

Mixture	1	2	3	4	5	6	7	8	9
% DNA (by mass)	100.0	57.1	40.0	28.6	16.7	10.0	7.1	4.8	1.6
% Protein (by mass)	0.0	42.9	60.0	71.4	83.3	90.0	92.9	95.2	98.4
Uncorrected DNA [conc] ng/µL	531.8	534.7	542.1	571.5	591.3	644.4	672.9	740.4	1097.6
Corrected DNA [conc] ng/µL	526.8	523.9	525.9	540.4	541.1	554.6	549.2	547.3	560.1
260/280 Purity Ratio	1.94	1.89	1.84	1.74	1.60	1.45	1.34	1.21	0.89
260/230 Purity Ratio	2.45	1.67	1.34	0.90	0.61	0.41	0.32	0.26	0.19
Acclaro Flag	No	No	No	No	⚠	⚠	⚠	⚠	⚠

Contaminants in nucleic acid samples

Protein is one of the significant contaminants in nucleic acid preparations that contributes to the absorbance at 260, inflates the concentration of the nucleic acid, and is usually detected by a decrease in the 260/280 purity ratio. The decrease in this ratio occurs because the amino acid residues (tryptophan, tyrosine, and phenylalanine) and the cystine disulfide bonds in protein absorb at 280 nm (Figure 1). The 260/280 ratio, a sensitive detection method for DNA contamination in protein preparations (Warburg, 1942)[1], was later adopted by the molecular biology community to detect protein contamination in nucleic acid preparations, but it has known limitations. Because the extinction coefficients of proteins are very small relative to those of nucleic acids, it takes a large amount of protein to affect the 260/280 purity ratio (Glasel, 1995, Huberman, 1995, and Manchester, 1995).[2-4] Nonetheless, scientists do see nucleic acid preparations with low 260/280 purity ratios.

The use of phenol to separate protein from nucleic acids has a history dating back to the 1950s, with the development of various protocols and formulations since then. However, the 1980s technique using a mixture of guanidinium thiocyanate, phenol, and chloroform to obtain highly pure, undegraded total RNA in a single step is the most popular[1-2]. Many RNA extraction kits modeled after this technique with different formulations are commercially available for cell lysis and protein denaturation. While calculating and assessing phenol contamination by one of the purity ratios mentioned above is traditional, this method is not very effective because phenol has an absorbance peak at 270 nm and the purity ratios of pure phenol are close to the acceptable ratios observed for pure DNA and RNA. Learn more about this in our next poster titled "Overcoming concentration calculation errors in the presence of phenol, guanidine, and other reagents".

MATERIALS AND METHODS

Double-stranded DNA (dsDNA) stock was prepared by diluting a salmon sperm DNA solution (Invitrogen™, #15632-011) in Tris-EDTA (TE) buffer (Fisher BioReagents™, pH 7.6, BP-2474-500). A protein stock was prepared by diluting a solution of bovine serum albumin (BSA, Sigma Aldrich®, #A7284) in TE buffer. The stock concentrations were determined on the NanoDrop One spectrophotometer against a TE blank. Mass calculations were made using the factor 50 ng-cm/µL for dsDNA and the extinction coefficient E1% 6.7 for BSA.

Five replicates for each of nine mixtures of DNA and protein were then prepared to generate the mixtures shown and measured on the NanoDrop One spectrophotometer against a TE blank. A fresh 1.5 µL aliquot of the appropriate mixture was used for each replicate. The software-calculated concentrations (corrected and original/uncorrected) and Acclaro Contaminant identity data were then used to generate the data sets presented (Table 1).

Figure 2. DNA concentration calculation comparisons. The average (N=5) is shown with error bars representing one SD from the mean for uncorrected (red), corrected (blue), actual dsDNA concentration (DNA-only control; dotted blue), and ±10% range from the average actual concentration (531.8 ng/µL; dotted green).

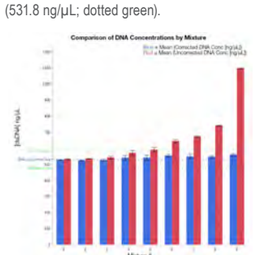

The original (uncorrected) concentrations versus the software-corrected concentrations were compared, and results are discussed below. Since mixtures 1–4 did not contain protein levels high enough to trigger an Acclaro Contaminant ID result, the corrected DNA concentration for mixtures 1 through 4 were determined by performing the Acclaro spectral analysis using the Thermo Scientific™ TQ Analyst™ software package.

RESULTS AND DISCUSSION

Table 1 presents the Acclaro Contaminant ID data obtained for the nine DNA/protein mixtures. As the level of contamination increases, the discrepancy between the corrected and the original (uncorrected) results becomes larger, emphasizing emphasizes how protein contamination can inflate an A260 concentration result. The software-corrected results show how the algorithm can quantitatively correct for these levels of protein contamination and provide a more accurate DNA concentration than the A260 value alone. Note that a large amount of protein contamination is required before a significant change in the 260/280 purity ratios is observed: samples with as much as ~72% protein by weight still have an acceptable 260/280 purity ratio. However, as the protein contaminant levels increase from ~72% to 98%, the 260/280 ratio drops steadily from 1.74 to 0.89.

Figure 3. Average purity ratios for dsDNA/Protein mixtures 1–9. 260/230 purity ratio (red line); 260/280 purity ratio (blue line).

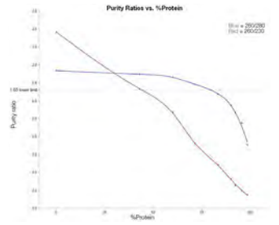

Figure 2 shows a comparison between the uncorrected and corrected DNA concentration data in the presence of different levels of protein contaminant. The presence of protein can inflate the original reported concentration. The data also shows that when the contaminant concentration is above ~72% protein by weight, Acclaro flags the sample and displays a corrected concentration (Table 1). The corrected DNA concentrations are within 10% of the result for the DNA only control. Mixture 9, which has the highest amount of protein contamination, shows the largest difference between the corrected and uncorrected concentration results. However, even with this extremely contaminated mixture where the protein represents >98% of the analyte mass in the sample, the software-corrected result brings the concentration result for mixture 9 to within 10% of the actual DNA concentration. These results were highly reproducible with standard deviations averaging under 1 ng/µL.

Figure 3 shows how purity ratios change with increasing levels of protein. As expected, as the percentage of protein contamination increases, the 260/280 purity ratio decreases. However, the amount of protein must be larger than 75% of the sample to observe a significant decrease in the 260/280 purity ratio (below 1.65), which is the lower limit generally accepted for use in downstream experiments. On the other hand, the 260/230 purity ratio steadily decreases as the percentage of protein in the mixture increases. These data also indicate that the 260/230 ratio may be a more sensitive indicator of protein contamination. The challenge of using this ratio to detect protein contamination is that many other common contaminants, such as common salt buffers, guanidine salts, and polysaccharides, can affect this ratio as well. Therefore, the 260/230 ratio alone cannot confirm protein contamination. The Acclaro Contaminant ID feature of the NanoDrop One spectrophotometer delivers a definitive advantage to the researcher by providing a corrected DNA concentration and by identifying contaminants present in a nucleic acid sample.

CONCLUSIONS

Experiments that use nucleic acids require that the concentration and purity of the sample is known. The UV-Vis method used for the quantification of nucleic acid preparations relies on the absorbance of nucleic acid molecules at 260 nm to determine the concentration of nucleic acids in solution. Contaminants, like protein, that are co-purified with nucleic acids can also absorb light in the UV region of the spectrum, which leads to overestimating the calculated nucleic acid concentration. Traditionally, purity ratios have been relied upon as an indication of the presence of contaminants in nucleic acid samples. "Out of range" purity ratios can indicate the presence of contaminants but cannot provide information on the identity and amount of the contaminant present. The Acclaro sample intelligence technology in the NanoDrop One spectrophotometer provides a chemometric approach for protein contaminant identification using UV spectrum analysis. This feature empowers researchers to 1) identify the type of protein contaminant present in their sample 2) determine the level of contamination and 3) obtain a corrected nucleic acid concentration. By using the Acclaro sample intelligence technology, you can make informed decisions on how to troubleshoot sample preparations to reduce contamination and how to proceed using a sample in downstream experiments.

REFERENCES

1. Warburg, O. and W. Christian. 1942. Isolation and crystallization of Enolase. *Z. Biochem.* 1942. 310:384-421.
2. Glasel, J.A. 1995. Validity of nucleic acid purities monitored by 260 nm/280 nm absorbance ratios. *Biotechniques* 18:62–63.
3. Huberman, J.A. 1995. Importance of measuring nucleic acid absorbance at 240 nm as well as at 260 nm and 280 nm. *Biotechniques* 18:636.
4. Manchester, K.L. 1995. Value of A260/A280 Ratios for the Measurement of Purity of Nucleic Acids. *Biotechniques* 19:208-210.

TRADEMARKS/LICENSING

ThermoFisher SCIENTIFIC

RETURN TO 'CONTENTS' PAGE

Qualification of nucleic acid samples for infectious disease research workflows

Patrick Brown and Brian Matlock - Thermo Fisher Scientific, 3411 Silverside Road Tatnall 100, Wilmington, DE 19810 USA

ABSTRACT

Reliable assays are a necessity for timely processing of samples that must be tested for SARS-CoV-2. To improve the quality and reliability of viral detection by the reverse transcription quantitative PCR (RT-qPCR) method, it is important to mitigate potential delays along the workflow. The Thermo Scientific™ Acclaro™ Sample Intelligence technology built in to the Thermo Scientific™ NanoDrop™ One Microvolume UV-Vis Spectrophotometer offers a set of tools that help provide accurate nucleic acid concentrations, identify many contaminants, and help prevent failed experiments.

Thermo Scientific NanoDrop One/One^{C}
Microvolume UV-Vis Spectrophotometer

INTRODUCTION

Testing considerations for SARS-CoV-2 samples

In early 2020, the World Health Organization published the genetic sequence for SARS-CoV-2, the virus that causes the COVID-19 disease. The disease spread and was classified as a pandemic on 11 March 2020. As of 3 August 2020, over 18 million individuals have tested positive for the virus around the world. Testing patients for the virus has been the primary focus for government organizations, hospitals, and private laboratories around the world. The Centers for Disease Control and Prevention describes several assays that can be used for the detection of the virus including RT-qPCR, antibody assays, electron microscopy, and more[1] (Figures 1 and 2). The Applied Biosystems™ TaqPath™ COVID-19 Combo Kit and several qPCR instruments were granted emergency use authorization by the U.S. Food and Drug Administration in Q2 2020[4].

Figure 1. Multiple SARS-CoV-2 detection workflows

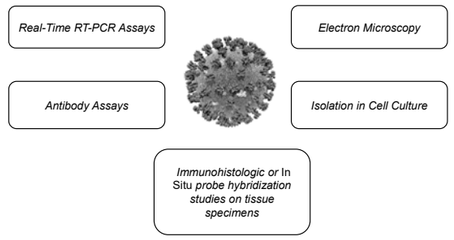

Figure 2. One SARS-CoV-2 workflow is a Real-Time RT-qPCR Assay. This figure is adapted from the CDC 2019-Novel Coronavirus (2019-nCoV) Real-Time RT-PCR Diagnostic Panel[2]. Note that the CDC guidelines do not mention nucleic acid quantification after RNA extraction or before qPCR amplification. The MIQE guidelines for minimum information for publication of quantitative real-time PCR experiments[3] do define nucleic acid quantity and A260/A280 purity as useful information for qPCR publication.

Importance of nucleic acid quantification

Reliable RT-qPCR assays demand careful experimental design, extensive QC, and transparent data analysis. In 2009, leaders within the qPCR field published the MIQE guidelines to improve the quality and reliability of experiments. An RT-qPCR assay includes two enzymatic steps. In the first step, RNA is converted to cDNA using reverse transcriptase. Normalizing the amount of RNA going into the reaction helps minimize variability in cDNA production, which can be crucial since RT reaction efficiencies can change with different RNA concentrations. During the second step, gene specific primers are used in combination with cDNA template to determine the relative expression compared to various reference genes. Reference genes are an important part of this reaction because they are used to normalize small differences in cDNA input. If there are large differences in cDNA amount, normalization based on reference genes can become problematic. The MIQE guidelines require input RNA quantity and purity are reported in publication.

Using NanoDrop One Spectrophotometers for qPCR workflows

The NanoDrop One Microvolume UV-Vis Spectrophotometer is trusted by scientists around the world for nucleic acid quantification of small volumes of sample. These instruments are built with Acclaro Sample Intelligence technology, which identifies the presence of many common contaminants in samples and calculates an approximate concentration of the contaminant. Common molecules found in nucleic acid extraction kits can overestimate analyte concentrations or denature qPCR polymerases. In either case, the qPCR experiment can fail. The Acclaro software provides corrected nucleic acid concentrations and identifies many common contaminants, to help minimize time spent troubleshooting and managing failed experiments, which are especially critical for mitigating issues under pandemic timelines.

RESULTS

Several CDC-approved nucleic acid extraction kits use guanidine thiocyanate (GuSCN) and guanidine HCl as part of their chemistries. If GuSCN contamination is present in a sample, it will not drastically change the reported absorbance value at 260 nm or the calculated nucleic acid concentration. However, it can denature qPCR polymerases. To illustrate this, we extracted RNA from mouse liver and spiked it with a GuSCN contaminant (Figure 3). We used absorbance at 260 nm to determine the analyte concentration and set-up qPCR based on the uncorrected value.

Figure 3. The effect of guanidine thiocyanate on nucleic acid spectra. The absorbance at 260 nm is unaffected by the presence of GuSCN, but the A260/A230 ratio may be impacted.

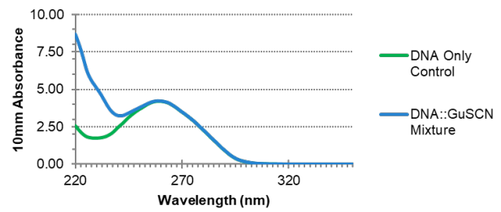

Because guanidine salt contamination can inhibit qPCR by denaturing polymerases, its presence could falsely elevate the cycle threshold (Ct) count. We measured Ct, noting that it increased with contaminant concentration and indicating that the reaction did not go as planned (Figure 4). We attribute this to the presence of guanidine salts that inhibit polymerases and block the reaction. Acclaro software built into the NanoDrop One can detect GuSCN in RNA samples and has features that can help prevent failed qPCR experiments (Figure 5 and Table 1).

Figure 4. Mouse Liver RNA spiked with GuSCN.

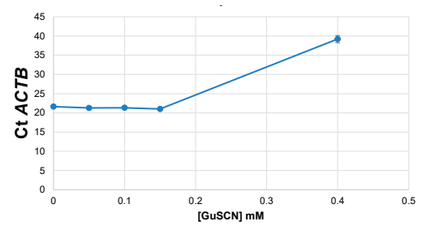

Figure 5. Acclaro technology contamination alerts. Acclaro technology A) flags an alert for a contaminant present in a dsDNA sample with an icon (⚠) and B) offers additional details about the protein contaminant in the sample that contributes to A260 that inflates dsDNA concentration. Acclaro provides uncorrected values and corrected values, where the protein contribution is subtracted from the original value to provide the corrected concentration.

A

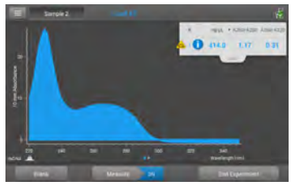

B

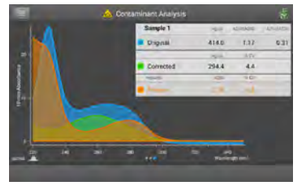

Table 1. Contaminant range detectable by Acclaro technology.

	dsDNA	RNA
Contaminants detected	• protein • phenol • guanidine HCl	• protein • phenol • guanidine SCN
Sample concentration range	0.5A-62.5A at 260 nm	0.5A-62.5A at 260 nm

CONCLUSIONS

The Acclaro Sample Intelligence technology in each NanoDrop One spectrophotometer helps improve confidence in sample assessment by identifying many common contaminants that could affect downstream RT-qPCR analysis. The algorithms provide corrected DNA or RNA concentration for each sample in under 8 seconds and calculate accurate A260/A280 and A260/A230 purity ratios. Having the ability to reduce costly delays from troubleshooting failed experiments by better understanding the original sample is a strongly desirable feature in time-sensitive assays.

REFERENCES AND NOTES

1. https://www.cdc.gov/sars/guidance/f-lab/assays.html
2. https://www.fda.gov/media/134922/download
3. https://www.ncbi.nlm.nih.gov/pubmed/19246619
4. **For Emergency Use Authorization (EUA) only. For prescription use only. For *in vitro* diagnostic use.**

TRADEMARKS, LICENSING & INTENDED USE

NanoDrop instruments are For Research Use Only. Not for use in diagnostic procedures. Applied Biosystems™ TaqPath™ COVID-19 Combo Kit and several qPCR instruments were granted Emergency Use Authorization by the U.S. Food and Drug Administration in April 2020.

ThermoFisher SCIENTIFIC

RETURN TO 'CONTENTS' PAGE

Blanking with high absorbing buffers such as RIPA negatively affects Protein A280 measurements

Patrick Brown and Brian Matlock - Thermo Fisher Scientific, 3411 Silverside Road Tatnall 100, Wilmington, DE 19810 USA

ABSTRACT

Thermo Scientific™ NanoDrop™ Microvolume UV-Vis Spectrophotometers are useful analytical tools for measuring the absorbance of small volumes of sample. Before making a sample measurement, the instrument must be blanked. Using the buffer in which the sample is suspended to making the blank measurement allows the software to account for the absorbance of the buffer solution and report an accurate analyte absorbance. The best buffers for UV-Vis spectroscopy have minimal absorbance at the analysis wavelength of the analyte. Here we show that blanking with a buffer that absorbs an appreciable amount of light leads to atypical absorbance measurements by diminishing the amount of light available for the sample measurement.

Thermo Scientific NanoDrop One/One^{C} Microvolume UV-Vis Spectrophotometer

INTRODUCTION

The most basic components of a UV-Vis spectrophotometer include a light source, the sample, and a detector. Light is illuminated through the sample and the amount of light transmitted to the detector is quantified. To calculate the absorbance, the amount of light transmitted through the sample must be compared to the amount of light transmitted through a reference substance (blank). Given these transmittances, one can calculate the absorbance of the sample with the equation:

$$\text{Absorbance} = -\log \frac{\text{Transmittance of Sample}}{\text{Transmittance of Blank}}$$

The blank measurement functionally removes the absorbance contributed to the sample by the buffer in which the sample is suspended. Essentially, this allows the software to subtract the buffer signal out of the sample signal to accurately report the analyte absorbance. The above equation can be rewritten by expanding the logarithmic term to obtain:

$$\text{Absorbance} = -[\log(\text{Transmittance of Sample}) - \log(\text{Transmittance of Blank})]$$

Blanking the instrument with the buffer in which the sample is suspended is generally recommended, but not all buffers are suitable for absorbance spectroscopy. A good buffer for blanking NanoDrop UV-Vis Spectrophotometers should have no more than ± 0.04 AU (absorbance units at a 10 mm pathlength) at the sample's analytical wavelength, which refers to the absorbance wavelength used to calculate the analyte concentration. When the software automatically selects the best pathlength, it uses the analytical wavelength.

Radioimmunoprecipitation assay buffer (RIPA) is frequently used in protein lysis preparations but absorbs a large amount of light near 280 nm. Here we examine the effects of blanking with RIPA on the measurement of protein absorbance at 280 nm.

RESULTS

The absorbance spectrum of RIPA buffer

When preparing to make absorbance measurements of an analyte in an untested buffer, performing a quick buffer analysis to determine how much light the buffer absorbs is recommended. Simply open the application in which you will make analyte measurements, blank the instrument with water, and measure your buffer as if it were a sample. As stated above, this buffer should have minimal absorbance.

Figure 1 shows the absorbance spectrum of RIPA after buffer analysis. At 280 nm, the analytical wavelength of proteins, RIPA absorbs approximately 22 AU By comparison, phosphate buffered saline (PBS) absorbs less than 0.01 AU at 280 nm (not shown).

Figure 1. Buffer analysis of RIPA. RIPA absorbs approximately 22 AU at 280 nm, the analytical wavelength of proteins.

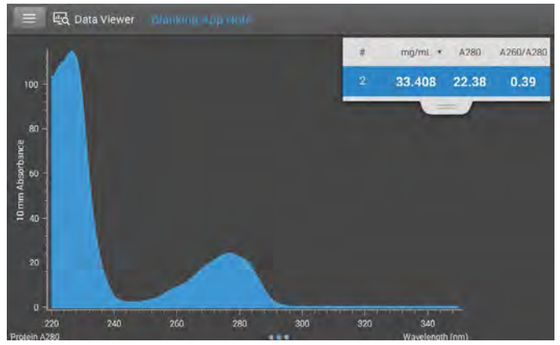

The Thermo Scientific™ NanoDrop™ One/One^{C} Microvolume UV-Vis Spectrophotometer operating software is built with the Thermo Scientific™ Acclaro™ Sample Intelligence Technology. One new technology is the blank absorbance verification feature. The software will not allow blanking with a buffer that has increased absorbance at the analysis wavelength and will instead display the message "Error: Blank solution absorbance too high. Clean both pedestals and blank again." This check exists because blanking with a highly absorbent buffer (such as RIPA) can negatively affect the absorbance measurement.

Measuring protein suspended in PBS and RIPA

The Protein A280 application measures the absorbance peak at 280 nm and calculates a protein concentration using the protein-specific extinction coefficient. The A280 peak appears due to the presence of tryptophan, tyrosine, and cysteine double bonds in the protein. PBS and RIPA solutions were prepared with the same weight of BSA and the same volume of solvent. Theoretically, the software should calculate the BSA concentration in both samples to be equivalent. Figure 2 displays the two resulting absorbance spectra: BSA suspended in PBS after the instrument was blanked with PBS (black spectrum) and BSA suspended in RIPA after blanking with RIPA (red spectrum). While the PBS spectrum appears as expected, the RIPA spectrum is distorted. BSA suspended in PBS displays a peak at 280 nm but BSA suspended in RIPA displays a trough at 280 nm. The difference in the absorbance at 280 nm between these two samples is approximately 88%.

Figure 2. Absorbance spectra of BSA suspended in PBS and RIPA. The black spectrum shows a pure BSA sample in PBS after blanking with PBS. The red spectrum shows a pure BSA sample in RIPA after blanking the instrument with RIPA.

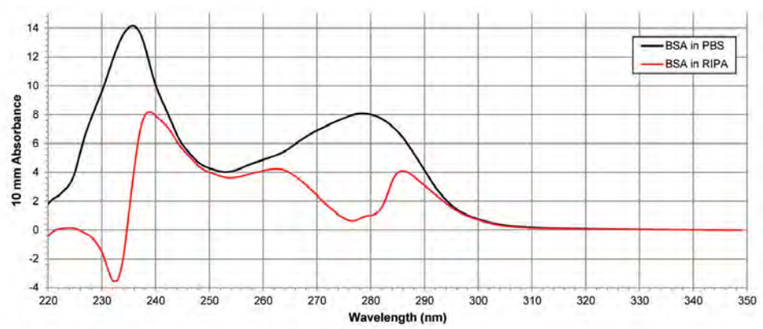

RIPA buffer limits the light intensity available for a sample measurement

The intensity check diagnostic confirms that the flash lamp and spectrometer are working within specifications. When running the intensity check, the user leaves the pedestals dry and the detector measures the amount of light produced by the lamp at a 1 mm pathlength. The software verifies the peaks in the xenon spectrum appear at their NIST-traceable locations.

Intensity checks were performed with deionized water, PBS, or RIPA on the pedestals. Figure 3 shows the resulting light intensities for these three solvents from 220 – 350 nm. While deionized water is highly transparent across the UV-Vis spectrum, RIPA absorbs a large amount of light, especially in the low UV region. Our data show the water (black solid line) and PBS (red dashes) intensities overlap, indicating that the light signal is not attenuated by PBS from 200 – 350 nm. In contrast, the intensity of RIPA (black dashes) shows a complete attenuation of light from 220 – 235 nm and 270 – 285 nm.

Figure 3. Flash lamp intensities with different solvents on the pedestal. The intensity of the lamp with PBS on the pedestals (red dashes) is the same as the intensity with water on the pedestals (black solid line). The signal with RIPA on the pedestals (black dashes) is attenuated near 280 nm and 220 – 235 nm.

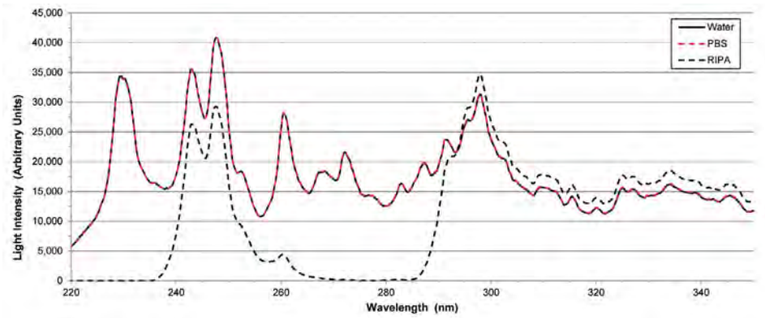

CONCLUSIONS

We recommend blanking NanoDrop UV-Vis Spectrophotometers using the same buffer in which the sample is suspended. For accurate analyte measurements, the blank buffer should have minimal absorbance near the analyte analytical wavelength for Protein A280 and other applications (e.g., Nucleic Acids). The buffer absorbance can be determined by performing a buffer analysis. In the case of RIPA buffer, it absorbs a large amount of light at the analytical wavelength of proteins. Absorbing this high amount of light limits the light available for the analyte measurement, a characteristic making RIPA a poor buffer choice for quantifying protein concentration using a direct 280 nm measurement. Rather than using the Protein A280 application, the use of a colorimetric assay application in the NanoDrop Spectrophotometer Software is recommended for measuring the concentration of proteins in RIPA. The operating software for full spectrum NanoDrop UV-Vis Spectrophotometers is hardcoded with applications to read the results of the Bradford, BCA, and Thermo Scientific™ Pierce™ 660 nm Protein Assays. This is discussed in detail in the technical document T112 – Influence of Buffer on Choice of Protein Quantification Method.

TRADEMARKS/LICENSING

ThermoFisher SCIENTIFIC

RETURN TO 'CONTENTS' PAGE

Resources

Safely accelerating drug development for brighter outcomes
A complete range of spectroscopy and materials characterization tools

Our comprehensive portfolio includes X-ray plasmon spectroscopy (XPS), energy-dispersive spectroscopy (EDS), Raman, Fourier-transform infrared (FTIR), near-infrared (NIR), X-ray diffraction (XRD), rheometers, and ultraviolet-visible (UV-Vis) spectroscopy. Using our state-of-the-art instruments ensures quality control across all steps and phases of your workflow and provides drug product consistency from initial formulations to large-scale production, employing fast, non-destructive methods.

Thermo Scientific Pharmaceutical Extruders allow drug formulation labs to produce consistent API dispersion from initial research through clinical trials and production, with three different sizes of twin-screw extruders that offer the hot melt extrusion (HME) and wet granulation (twin-screw granulation or TSG) capabilities.

When you need additional help, our services and support teams can provide repair of critical instruments and after-sales service and support.

View our brochure today.

On-demand webinars

A wide range of educational webinars that can be viewed on demand as your time permits. The webinars offer topics covering the full pharmaceutical workflow from research & discovery, development, manufacturing as well as compliance and data integrity.

Quality assurance and data integrity from an auditors' viewpoint

Hear directly from industry auditors as they discuss the current regulatory framework for good manufacturing practice (GMP), including data integrity, validation and qualification for computerized systems in regulated laboratories.

Biodegradable Long-acting Injectable Implants Prepared by Hot Melt Extrusion

Development and manufacturing of injectable implants often involves polymers as a matrix which makes twin-screw extrusion a perfect technology for their development. Nevertheless, it is a comparatively new technology, and much can still be learned about the applicability and benefits of twin-screw extrusion. This seminar aims to give an introduction as well as real-life examples of what to look out for when entering this field of pharmaceutical manufacturing.

Patheon Experience: Overcoming Challenges to Ensure Data Integrity and Standardization

Hear from Patheon Pharma Services about their requirements for compliance and data integrity, and how they overcame the challenges encountered when evaluating and implementing new equipment. Adhering to 21 CFR Part 11 is an important part of compliance but does not guarantee data integrity. Learn how and why Patheon implemented both FTIR Spectroscopy and a Chromatography Data System in different areas of their workflow to meet data integrity needs and the importance of these to the business.

Lean Manufacturing with Raman Spectroscopy for Biopharmaceutical Production

Biopharmaceutical manufacturers are increasing their testing regimes and increasing their efforts to raise current production levels. However, due to bottlenecks in current testing procedures, it's not always easy to shorten testing times.

Shailesh Karavadra, from Thermo Fisher Scientific, addresses the role of the Raman spectroscopy in the rapid release of raw materials through identity testing and real-time release testing of final products such as vaccines, hormones and monoclonal antibodies. Gain further insight into how traditional testing can be replaced with Raman spectroscopy.

Improving quality of bacterial culture and oligonucleotides with UV/Vis spectroscopy to accelerate mRNA vaccine production

Bacterial growth rate and nucleotides are the main components that impact the manufacture mRNA vaccines for COVID-19 prevention. In this webinar, Naimish Sardesai of Thermo Fisher Scientific explains how bacterial growth rate influences gene expression by acting on both sides of the mRNA equilibrium: synthesis and degradation. Naimish Sardesai will also discuss how Thermo Fisher Scientific's GENESYS and Evolution series UV/Vis spectrophotometers can be used to evaluate and achieve optimum bacterial culture growth rate, and measure oligonucleotide quality to ensure vaccines produced are not contaminated.

Predicting the crystalline nature of Active Pharmaceutical Ingredients (APIs)

Prof. Gérard Coquerel, head of the Separative Sciences and Methods Laboratory at the University of Rouen Normandy, will illustrate how the precise identification of solid phases and their crystallinity are important for the design of drying, the storage conditions, and the repeatability of the solid transformations regarding APIs, as well as the identification of non-stoichiometric solids and the possible presence of polymorphs of hydrates and anhydrates.

5-Part OnDemand Webinar Series: Pharmaceutical Analysis with Spectroscopy, Extrusion and XRD

Explore this free series of 5 webinars on pharmaceutical applications and concerns ranging from making implants to API domains and compliance. Topics include:

- Instrument Systems Take on Burden of Compliance
- Effective Imaging for Identification and Sizing API Domains
- NIR to the Rescue: Production Efficiency and Cost Savings for Pharma
- Injectable Implants: Manufacturing Advanced Medicines with Hot Melt Extrusion
- Capable and Compliant XRD in Pharmaceuticals

ThermoFisher
SCIENTIFIC

Resources on thermofisher.com

Pharma & Biopharma:
thermofisher.com/brighteroutcomes

Drug Formulation & Manufacturing:
thermofisher.com/drugformulation

Molecular Spectroscopy:
thermofisher.com/spectroscopy

Nucleic Acid Quantitation:
thermofisher.com/nanodrop

To consult with an expert in tools for pharmaceutical formulation and analysis, please visit:
thermofisher.com/specinquiry